MIA: A Framework for Certifiably Robust Time-Series Classification and Forecasting Against Temporally-Localized Perturbations

Anonymous authors
Paper under double-blind review

Abstract

Recent literature demonstrates that times-series forecasting/classification are sensitive to input perturbations. However, the defenses for time-series models are relatively under-explored. In this paper, we propose **M**asking **I**mputing **A**ggregation (MIA), a plug-and-play framework to provide an arbitrary deterministic time-series model with certified robustness against temporally-localized perturbations (also known as ℓ_0-norm localized perturbations), which is to our knowledge the first ℓ_0-norm defense for time-series models. Our main insight is to let an occluding mask move across the input series, guaranteeing that, for an arbitrary localized perturbation there must exist at least one mask that completely occlude the perturbed area, so that the prediction on this masked series is certifiably unaffected. MIA is flexible as it still works even if we only have the query access to the pretrained model. To further validate the superior effectiveness of MIA, we specifically compare MIA to two baselines extended from prior randomized smoothing approaches. Extensive experiments show that MIA yields stronger robustness.

1 Introduction

Time series forecasting/classification (TSF/TSC) have been widely applied to help businesses make informed decisions and plans (Miyato et al., 2017; Zhou et al., 2019; Schlegl et al., 2019; Park et al., 2018). However, a wide range of literature demonstrate that time-series models are vulnerable to adversarial input perturbations (Connor et al., 1994; Gelper et al., 2010; Ding et al., 2022; Yang et al., 2020; Dang-Nhu et al., 2020; Oregi et al., 2018; Han et al., 2020), e.g., an elaborately designed imperceptible perturbation could control the prediction (Karim et al., 2020; Fawaz et al., 2019). So far related literature is mainly focusing on detecting the outliers (Ruff et al., 2018; Yairi et al., 2017), the adversarial robustness of time-series models is relatively under-explored, especially ℓ_0-norm robustness, e.g., (Yoon et al., 2022) only explore the ℓ_2-norm adversarial robustness for probabilistic forecasting models. In the present work, we focus on the robustness against temporally-localized perturbations, as we notice there already exists corresponding powerful attacks (Yang et al., 2022).

Generally, defenses can be divided into two types, heuristic defenses and certified defenses. Heuristic defense can yield better empirical robustness but lack robustness guarantees. From the experience on image classification (Athalye et al., 2018; Carlini & Wagner, 2017; Athalye & Carlini, 2018), the heuristic defenses would be useless when confronted with the newly designed adaptive attacks, e.g., Athalye et al. (2018) leverage Backward Pass Differentiable Approximation technique to successfully circumvent almost all the heuristic defenses at that time. To end such a "cat and mouse" game between the adaptive attacks and the heuristic defenses, the concept of certified defense is proposed, with unbreakable robustness certificates.

Current certified defenses can produce robustness certificates but often require the user to retrain the base model from scratch, e.g., Yoon et al. (2022); Li et al. (2020); Cohen et al. (2019) retrain the base model as these defenses do perform poorly on naturally-trained models. The requirement for retraining could bring additional challenges when it comes to the real-world deployments. In addition, the certified defenses on sequence-based data are quite under-explored, since almost all the certified defenses are focusing on matrix-based data (e.g. image).

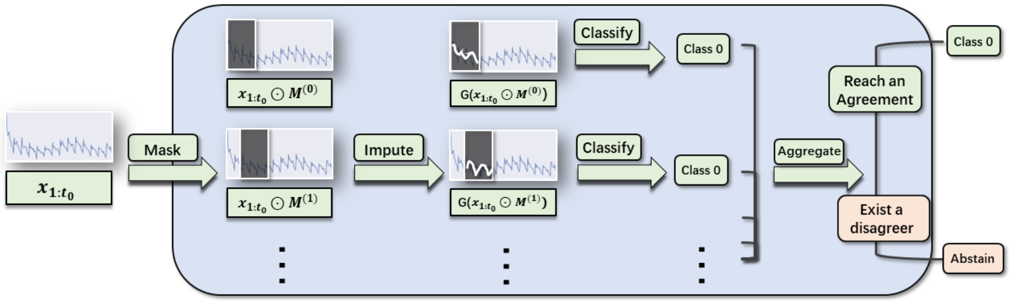

Figure 1: Overview of MIA pipeline. Inputted a series $\mathbf{x}_{1:t_0}$, MIA first masks different periods of $\mathbf{x}_{1:t_0}$ to construct the masked series $\mathbf{x}_{1:t_0} \odot \mathrm{M}^{(k)}, k = 0, \ldots, M$. Then MIA imputes the masked series with the imputation model $G(\cdot)$. We classify the imputed series with the pretrained model. If the predictions of all the imputed series are *Class 0*, MIA will return *Class 0* with the robustness guarantee that the output is clean, otherwise MIA will return **Abstain**.

To address these issues, in this paper, we propose **M**asking **I**mputing **A**ggregation (MIA), a flexible framework to arm an arbitrary TSF/TSC deterministic model with robustness certificates against temporally-localized perturbations. Different from the requirement for retraining in prior defenses, MIA only an imputation model for recovering the masked areas, which can be easily learned in an unsupervised setting. Specifically, MIA works as follows: 1) **masking:** MIA first masked series via sliding a mask through the input series; 2) **imputing:** MIA imputes the masked series with the imputation model; 3) **aggregation (checking agreement):** MIA only returns the the class if the pretrained model outputs the same for all the imputed series, otherwise returns Abstain. With the above three steps, we can guarantee that all the predictions from MIA is clean. Furthermore, we compare MIA to two baselines extended from randomized smoothing, as we notice that randomized smoothing has achieved a widespread success in defending different adversarial attacks. **The contributions are:**

1) We propose MIA, a plug-and-play framework to arm an arbitrary TSF/TSC model with certified robustness against temporally-localized perturbations, which is to our knowledge the first ℓ_0-norm certified defense in time series domain.

2) We propose randomized masked training, a specialized training algorithm for training the imputation model of MIA, to further boost the performance of MIA.

3) We compare MIA to two baseline methods comprehensively on three aspects. 1) robustness: extensive experiments on different datasets validate that superior robustness of MIA. 2) Practicality: MIA is stronger as it is plug-and-play and do not require retraining. 3) Inference cost: the inference time of MIA is comparable to the time cost of two baselines.

2 Related Work

Heuristic defenses for time-series models. Prior works on robust TSF/TSC can be divided into two general categories: outlier detection and deep learning. The former is to filter the outliers in a statistical way, including k-Means clustering (Yang et al., 2017), one-class SVM clustering (Schölkopf et al., 2001), Kalman filters (de Bézenac et al., 2020) and support vector data description (Tax & Duin, 2004). The latter leverages the strong representation ability of neural networks to recover the perturbed series, including robust feature-based approaches (Guo et al., 2016; Yang & Fan, 2022), reconstruction-based methods (Li et al., 2021; 2019; Xu et al., 2018; Schlegl et al., 2019), GNN-based methods (Zhao et al., 2020; Deng & Hooi, 2021), association discrepancy (Xu et al., 2022), LSTM-based methods (Hundman et al., 2018; Tariq et al., 2019). However, these empirical methods lack robustness guarantees, hinting that they would be meaningless once a new adaptive attack is found. For that reason, certified defenses are crucial because their mathematical robustness certificates are permanently unbreakable.

Certified adversarial defenses. In the field of image classification, there has been much work on the certified defenses, including randomized smoothing (Cohen et al., 2019; Salman et al., 2020), convex polytope (Wong & Kolter, 2018), CROWN-IBP (Zhang et al., 2019) and Lipschitz bounding (Cisse et al., 2017). Among them, the ℓ_0-norm defenses include derandomized smoothing (Levine & Feizi, 2020a), randomized ablation (Levine & Feizi, 2020b; Zhang et al., 2020) and a series of mask-based defenses (Xiang & Mittal, 2021; McCoyd et al., 2020; Han et al., 2021; Xiang et al., 2021; 2022). *In stark contrast, the certified defenses for time-series data are rarely explored.* To our knowledge, (Yoon et al., 2022) and (Li et al., 2020) are the only two defenses that produce ℓ_2-norm robustness certificates, but a common downside is that they both additionally require retraining the base model over Gaussian augmented samples, which imposes a large amount of additional training costs.

3 Preliminaries

Time series classification (TSC). The time series classification is modeled as: inputted a t_0-length series (denoted by $\mathbf{x}_{1:t_0} = [x_1, x_2, \ldots, x_{t_0}]$), TSC model returns a class $f(\cdot) : \mathbf{x}_{1:t_0} \to y$.

Time series forecasting (TSF). Given the "past observations" $\mathbf{x}_{1:t_0}$, the forecasting model returns the "future values" $f(\cdot) : \mathbf{x}_{1:t_0} \to \mathbf{x}_{t_0+1,t_0+\tau}$. In this paper we mainly focus on the classic and commonly studied short-term forecasting setting (Ke et al., 2017), which is to forecast a single time point $f(\cdot) : \mathbf{x}_{1:t_0} \to \mathbb{R}$ (not necessarily the next point x_{t_0+1}). The short-term forecasting problem is sufficiently representative as the problem of long-term forecasting $f(\mathbf{x}_{1:t_0}) \to \mathbf{x}_{t_0+1:t_0+\tau}$ can be decomposed into τ short-term forecasting subproblems, in which the i-th ($i = 1, \ldots, \tau$) forecaster predicts the $(t_0 + i)$-th time point. We discuss the multivariate tasks later in this paper.

Definition 1 (Temporally-localized perturbation $\boldsymbol{\delta}_{[t_{\text{adv}}+1:t_{\text{adv}}+L_{\text{adv}}]}$)**.** In a temporally-localized perturbation attack, the adversary is allowed to *perturb an arbitrary subseries w.r.t. the given ℓ_0-norm constraint*. Let L_{adv} be the ℓ_0-norm constraint on the localized perturbation. We can formulate all the perturbed series w.r.t. the ℓ_0-norm constraint as follows:

$$\begin{aligned} &\mathbf{x}_{1:t_0} + \boldsymbol{\delta}_{[t_{\text{adv}}+1:t_{\text{adv}}+L_{\text{adv}}]} \\ =&\mathbf{x}_{1:t_0} + [0, \ldots, 0, \delta_{t_{\text{adv}}+1}, \ldots, \delta_{t_{\text{adv}}+L_{\text{adv}}}, 0, \ldots, 0] \\ =&[x_1, \ldots, \underbrace{x_{t_{\text{adv}}+1} + \delta_{t_{\text{adv}}+1}, \ \ldots, \ x_{t_{\text{adv}}+L_{\text{adv}}} + \delta_{t_{\text{adv}}+L_{\text{adv}}}}_{\text{Perturbed subseries}}, \ \ldots, x_{t_0}] \end{aligned} \tag{1}$$

where unbold δ_t refers to the single perturbation value added to the t-th time point. $t_{\text{adv}} + 1$ and $t_{\text{adv}} + L_{\text{adv}}$ refer to the starting point and the ending point of the perturbation respectively, which explicitly restricts its ℓ_0 norm as $\|\boldsymbol{\delta}_{[t_{\text{adv}}+1:t_{\text{adv}}+L_{\text{adv}}]}\|_{\ell_0} = (t_{\text{adv}} + L_{\text{adv}}) - (t_{\text{adv}} + 1) + 1 = L_{\text{adv}}$.

Significance of temporally-localized perturbation. Temporally-localized perturbation is especially representative in real-world scenarios. Temporally-localized perturbation can represent *short-term volatility* and *local anomaly*, both of which can be regarded as the normal data added with temporally-localized perturbation. The resistance to short-term volatility is important in long-term forecasting/prediction, in which the long-term value is considered unaffected by the short-term volatility. A typical example is the well-known investment philosophy, "Value Investing" (Piotroski, 2000), where the "intrinsic value" of a business is considered to be robust against short-term volatility. Moreover, the detection of local anomaly is practically useful in real-world scenarios. For instance, detecting a subsequent time interval of abnormal heart rate in electronic health records is a problem of local anomaly detection. We can also adopt the method of detecting temporally-localized perturbation for detecting the abnormal network traffic for IoT Time-Series Data. Furthermore, to highlight the risk of temporally-localized perturbations, we empirically show how much a ℓ_0-norm perturbation can change the output of an undefended forecaster in Appendix. We also compare the attacking performance of ℓ_0-norm perturbation to ℓ_0-norm perturbation, and the empirical results suggest that forecasting models might be more sensitive to ℓ_0-norm perturbations.

4 Proposed Framework: Masking Imputing Aggregation

4.1 Pipeline Overview

MIA includes three steps: 1) masking; 2) imputing; 3) aggregation (checking agreement).

1. **Masking.** We denote a mask by $\mathrm{M}_{[u:v]}$, where $\mathbf{x}_{1:t_0} \odot \mathrm{M}_{[u:v]}$ is replacing the values of $\mathbf{x}_{u:v}$ among $\mathbf{x}_{1:t_0}$ with zeros. Let L_{mask} be the size of the mask. Inputted a series $\mathbf{x}_{1:t_0}$ and the ℓ_0 norm of the temporally-localized perturbation L_{adv}, we slide the mask thorough the input series with the step size $\alpha = L_{\text{mask}} - L_{\text{adv}} + 1$, and then obtain the following masked series[1] :

$$\begin{aligned} &\mathbf{x}_{1:t_0} \odot \mathrm{M}_{[1+k\alpha\,:\,\min(L_{\text{mask}}+k\alpha, t_0)]}, \ k = 0, \ldots, \lceil (t_0 - L_{\text{mask}})/\alpha \rceil \\ &\text{where} \quad \alpha = L_{\text{mask}} - L_{\text{adv}} + 1 \end{aligned} \tag{2}$$

[1] $\lceil c \rceil$ returns the smallest integer larger than or equal to c

Algorithm 1: Algorithm of Masking Imputing Aggregation.

Input: The pretrained TSF/TSC model $f(\cdot)$, the imputation model $G(\cdot)$, the input series $\mathbf{x}_{1:t_0}$, the mask size L_{mask}, the length of temporally-localized perturbation L_{adv}, the discretization parameter Δ for TSF task.

Compute the step size of masking $\alpha \leftarrow L_{\text{mask}} - L_{\text{adv}} + 1$;

Generate the masked series via sliding the L_{mask}-size mask $\mathbf{x}_{1:t_0} \odot \mathrm{M}_{[1+k\alpha:\min(t_0, L_{\text{mask}}+k\alpha)]},\ k = 0, \ldots, \lceil (t_0 - L_{\text{mask}})/\alpha \rceil$;

Utilize the imputation model to impute the masked series $\mathbf{x}_{1:t_0}^{(k)} = G(\mathbf{x}_{1:t_0} \odot \mathrm{M}_{[1+k\alpha:\min(t_0, L_{\text{mask}}+k\alpha)]})$;

Compute the output (denoted by $y^{(k)}$) for each imputed series, as follows:

$$y^{(k)} = \begin{cases} f(\mathbf{x}_{1:t_0}^{(k)}) & \text{for TSC task} \\ f_{\text{dis}}(\mathbf{x}_{1:t_0}^{(k)}) & f_{\text{dis}}(\cdot)\text{for TSF task} \end{cases}$$

\# $f_{\text{dis}}(\mathbf{x}_{1:t_0}^{(k)})$ is computed as Eq. (5);

if $y^{(0)} = y^{(1)} = \ldots = y^{(k)}$ **then**

  Output: $y^{(0)}$.

else

  Output: Abstain.

We set the step size to $L_{\text{mask}} - L_{\text{adv}} + 1$ for guaranteeing all the temporally-localized perturbations of L_{adv} can be covered. $\min(L_{\text{mask}} + k\alpha, t_0)$ is to prevent the mask from exceeding t_0.

2. **Imputing.** Our second step is to recover the masked values with the imputation model $G(\cdot)$:

$$\mathbf{x}_{1:t_0}^{(k)} = G(\mathbf{x}_{1:t_0} \odot \mathrm{M}_{[1+k\alpha:\min(t_0, L_{\text{mask}}+k\alpha)]}) \quad k = 0, 1, \ldots, \lceil (t_0 - L_{\text{mask}})/\alpha \rceil \tag{3}$$

This step is to make $\mathbf{x}_{1:t_0}^{(k)}$ approximate the normal time series, so that the pretrained model could perform similarly on these imputed series. We discuss $G(\cdot)$ later this section.

3. **Aggregation (Checking Agreement).** We input the imputed series $\mathbf{x}_{1:t_0}^{(k)}$ into the pretrained model $f(\cdot)$. If the pretrained model's ouputs on all $\mathbf{x}_{1:t_0}^{(k)}$ reach agreement unanimously, MIA classifier $f_{\text{MIA}}(\mathbf{x}_{1:t_0})$ will output this unanimously approved label/prediction, otherwise output **Abstain** to alert that the input series might have been attacked by the temporally-localized perturbations.

$$f_{\text{MIA}}(\mathbf{x}_{1:t_0}) = \begin{cases} f(\mathbf{x}_{1:t_0}^{(0)}) & f(\mathbf{x}_{1:t_0}^{(0)}) = f(\mathbf{x}_{1:t_0}^{(1)}) = \ldots = f(\mathbf{x}_{1:t_0}^{(\lceil (t_0 - L_{\text{mask}})/\alpha \rceil)}) \\ \textbf{Abstain} & \text{Otherwise} \end{cases} \tag{4}$$

Discretization technique for MIA on TSF. We note that TSF models are impossible to forecast exactly the identical value on different series, so that MIA would output **Abstain** all the time on TSF. To address this, we substitute the original pretrained forecaster $f(\cdot)$ with its discretized version $f_{\text{dis}}(\cdot)$ in Eq. (4), where $f_{\text{dis}}(\mathbf{x}_{1:t_0}^{(k)}), k = 0, \ldots, \lceil (t_0 - L_{\text{mask}})/\alpha \rceil$ compute as follow:

$$f_{\text{dis}}(\mathbf{x}_{1:t_0}^{(k)}) = \Delta \cdot \lfloor f(\mathbf{x}_{1:t_0}^{(k)})/\Delta \rfloor \tag{5}$$

where Δ is a discretization parameter that controls the trade-off between the discretization error and the success rate of achieving agreement. As Δ decreases, the discretized forecasts retain more information from the original forecasts while the agreement rate decreases. If we take $\Delta = 0.5$, $f_{\text{dis}}(\mathbf{x}_{1:t_0}^{(k)})$ is to round up the value of $f_{\text{dis}}(\mathbf{x}_{1:t_0}^{(k)})$ to the nearest integer.

4.2 Discussion on the mask size L_{mask}.

The only requirement of **Masking (Step 1)** is to ensure *for an arbitrary temporally-localized perturbation of* L_{adv}, *there always exists a mask to occlude that perturbation*. Thus a prerequisite is $L_{\text{mask}} \geq L_{\text{adv}}$. We can control the trade-off between the the imputation quality and the inference cost with L_{mask}. As we increase L_{mask}, the imputation quality will decrease since the number of missing values increases. Meanwhile, the number of masked series decreases subsequently, so the inference cost is reduced. In the extreme case where $L_{\text{mask}} = t_0$ where the masked series are all equal $\mathbf{0}_{1:t_0}$, MIA always outputs $f(G(\mathbf{0}_{1:t_0}))$ regardless of the input series. The imputation quality is extremely poor and the inference cost is the smallest. **The practical implementation of MIA is showed in Algorithm 1.**

Remark 1 (MIA on Probabilistic Models)**.** We notice a line of time-series forecasting models are probabilistic (e.g., DeepAR (Salinas et al., 2020)), which models the forecasted value $f(\mathbf{x}_{1:t_0})$ as a random distribution $q[y \mid \mathbf{x}_{1:t_0}]$ rather than a single value, as follows:

$$f(\mathbf{x}_{1:t_0}) = \mathbb{E}_{q[x_{t_0+1}|\mathbf{x}_{1:t_0}]}\left[x_{t_0+1}\right] \tag{6}$$

The exact forecasting value of probabilistic models is inaccessible (prior works perform Monte-Carlo inference for approximation). which makes applying MIA to probabilistic models challenging. Although we can utilize Clopper-Pearson method (Clopper & Pearson, 1934) to estimate the discretized forecasts $f_{\text{dis}}(\mathbf{x}_{1:t_0})$ with a confidence level, the inference cost would be expensive for confidence interval estimation. [2]

4.3 Robustness Certificate of MIA

Proposition 1 (Robustness Certificate of MIA)**.** The forecast/label (not **Abstain**) returned by Algorithm 1 cannot be changed by any temporally-localized perturbation whose ℓ_0 norm is no larger than L_{adv} (see proof in Appendix).

Remark 2 (Robustness Certificate)**.** The robustness certificate is for $f_{\text{MIA}}(\mathbf{x}_{1:t_0})$ rather than $f(\mathbf{x}_{1:t_0})$ because it is almost impossible to derive the certificate for a pretrained model without any requirement. Our aggregation does not allow any tolerance because the certificate would not hold once a disagreement is allowed. Note that, with **Masking (Step 1)**, we can guarantee there exists a masked series that is unaffected, and all other masked series retain the perturbed area. If we allow a disagreer, the ensemble prediction would be totally under the adversary's control, because all except one masked series are perturbed (the only one not affected would become the disagreer). We point out that the certificate also holds for multivariable TSC/TSF. We can easily apply MIA to multivariable tasks through repeating **Masking (Step 1)** and **Imputing (Step 2)** on each variable.

4.4 Training Imputation Model $G(\cdot)$

The performance of MIA highly depends on the imputation model $G(\cdot)$. We notice that there already exists much work on time series imputation (Cao et al., 2018; Du et al., 2022; Moritz & Bartz-Beielstein, 2017; Fortuin et al., 2020; Cao et al., 2018; Luo et al., 2019; Yozgatligil et al., 2013). However, all these imputation models aim to recover the discrete missing values, which is not we want. To train an imputation model to recover consecutive missing values, we propose *randomized masked training algorithm*, which minimizes the MSE loss over the masked noisy series, as follows:

$$\mathbb{E}_{\boldsymbol{\delta}_{[1:t_0]}\sim\mathcal{N}(0,\sigma^2)}\ \frac{1}{C+1}\sum_{k=0}^{C}\|G\left((\mathbf{x}_{1:t_0}+\boldsymbol{\delta}_{[1:t_0]}\right)\odot M_{[1+k\alpha:\min(L_{mask}+k\alpha,t_0)]})-\mathbf{x}_{1:t_0}\|_2^2 \tag{7}$$

where $C = \lceil (t_0 - L_{mask})/\alpha \rceil$ and $\boldsymbol{\delta}_{[1:t_0]} \sim \mathcal{N}(0, \sigma^2)$ is a Gaussian noise series, of which each entry is *i.i.d.* sampled from Gaussian distribution. We specifically add Gaussian noise is to make the imputation model robust to the random noise and avoid overfitting, since prior works (Foster et al., 1992; Passalis et al., 2021; Hwang et al., 1998) show the time series data is generally noisy. We emphasize that we do not add any noise in inference stage.

4.5 Comparison to Randomized Smoothing Defenses

Randomized smoothing (Cohen et al., 2019) is a well-know model-agnostic method in the field of certified defenses, which has been applied to defend various types of attacks and achieves superior certified robustness in their respective fields. Comparing MIA to randomized smoothing can better demonstrate the advance of our method. We extend two image-specific randomized smoothing defenses, Derandomized Smoothing (Levine & Feizi, 2020a) and Randomized Ablation (Levine & Feizi, 2020b) to the time series domain, as the baselines.

Derandomized smoothing for time-series models. In the time-series version of DS, given a time series $\mathbf{x}_{1:t_0}$ and the base classifier $f(\cdot)$, DS (denoted by f_{DS}) classifies as follows[3]:

$$f_{\text{DS}}(\mathbf{x}_{1:t_0}) = \arg\max_{y\in\mathcal{Y}}\left[\sum_{\mathbf{x}_{\text{sub}}\in\text{Sub}(\mathbf{x}_{1:t_0},\eta)}\mathbb{I}\{f(\mathbf{x}_{\text{sub}})=y\}\right] \tag{8}$$

[2]We notice that a recent work (Yoon et al., 2022) derives robustness certificate for probabilistic forecasters, but our definitions of robustness are different. Yoon et al. (2022) bounds the local Lipschitz constant, while our objective is much stricter, aiming to guarantee the forecast is invariant under the perturbation.

[3]$\mathbb{I}\{\}$ is the indicator function.

Table 1: (DistalPhalanxTW) Comparison among three defenses on a TSC dataset.

Defense	1 %	2 %	3 %	4 %	5 %	6 %	7 %	8 %	9 %	10 %
MIA ($L_{\text{mask}} = 10\%$)	**67.3%**	**66.3%**	**67.3%**	**67.3%**	**66.3%**	**64.4%**	**66.3%**	**64.4%**	**64.4%**	**63.4%**
DS ($\eta = 10\%$)	28.1%	28.1%	28.1%	28.1%	28.1%	28.1%	28.1%	28.1%	28.1%	28.1%
RA ($\eta = 10\%$)	5.8%	5.8%	5.8%	5.8%	5.8%	5.8%	5.8%	5.8%	5.8%	5.8%
MIA ($L_{\text{mask}} = 15\%$)	**62.4%**	**65.3%**	**65.3%**	**64.4%**	**64.4%**	**62.4%**	**63.4%**	**65.3%**	**63.4%**	**64.4%**
DS ($\eta = 15\%$)	30.2%	30.2%	30.2%	30.2%	30.2%	30.2%	30.2%	30.2%	30.2%	30.2%
RA ($\eta = 15\%$)	9.4%	9.4%	9.4%	9.4%	9.4%	9.4%	9.4%	9.4%	9.4%	9.4%

where $\text{Sub}(\mathbf{x}_{1:t_0}, \eta)$ consists of the subsequences $\mathbf{x}_{1:\eta}, \mathbf{x}_{\eta+1:2\eta}, \mathbf{x}_{2\eta+1:3\eta}, \ldots, \mathbf{x}_{t_0-\eta+1,t_0}$. We first let the base classifier make predictions on these subsequences, and then $f_{\text{DS}}(\mathbf{x}_{1:t_0})$ outputs the majority label. The prediction is robust if

$$\sum_{\mathbf{x}_{\text{sub}} \in \text{Sub}(\mathbf{x}_{1:t_0}, \eta)} \mathbb{I}\{f(\mathbf{x}_{\text{sub}}) = \hat{y}\} - \max_{y \neq \hat{y}} \sum_{\mathbf{x}_{\text{sub}} \in \text{Sub}(\mathbf{x}_{1:t_0}, \eta)} \mathbb{I}\{f(\mathbf{x}_{\text{sub}}) = y\} > 2(\eta + L_{\text{adv}} - 1) \tag{9}$$

Randomized ablation for time-series models. RA (denoted by $f_{\text{RA}}(\cdot)$) classifies as follows:

$$f_{\text{RA}}(\mathbf{x}_{1:t_0}) = \arg\max_{y \in \mathcal{Y}} \left[\Pr_{\mathbf{x}_{\text{sub}} \sim \text{Sample}(\mathbf{x}_{1:t_0}, \eta)} [f(\mathbf{x}_{\text{sub}}) = y] \right] \tag{10}$$

where $\mathbf{x}_{\text{sub}} \sim \text{RA}(\mathbf{x}_{1:t_0}, \eta)$ is to randomly sample η time points without replacement to construct the subseries $\mathbf{x}_{\text{sub}}$, and ablate all other points. $f_{\text{RA}}(\mathbf{x}_{1:t_0})$ returns the label that $f(\cdot)$ is most likely to classify $\mathbf{x}_{\text{sub}}$ as. $\hat{y} = f_{\text{RA}}(\mathbf{x}_{1:t_0})$ is robust if

$$\Pr_{\mathbf{x}_{\text{sub}} \sim \text{Sample}(\mathbf{x}_{1:t_0}, \eta)} [f(\mathbf{x}_{\text{sub}}) = \hat{y}] > \frac{3}{2} - \frac{\binom{t_0 - L_{\text{adv}}}{\eta}}{\binom{t_0}{\eta}} \tag{11}$$

Comparison to DS and RA. We note that the pretrained models of DS and RA make predictions on subseries $f(\mathbf{x}_{\text{sub}})$ instead of normal series. Since the data distribution of the subseries are fundamentally different from the normal data, we can expect that these two defenses would perform poorly on the naturally-trained models. Therefore, we need to train the base classifiers from scratch on the subseries. In stark contrast, MIA is a plug-and-play framework that can be directly applied to TSF/TSC pretrained models. In MIA, the main cost of training stage is preparing the imputation model. We point out that the imputation model of MIA can be trained in an unsupervised manner, saving us from labeling the data. Furthermore, we empirically show that MIA attains a significantly better robustness than DS and RA in Section 5.

5 Experiments

Experimental setup. We evaluate MIA on both TSC and TSF datasets. TSF includes Exchange Rate, Traffic and UCI Electricity (Alexandrov et al., 2019), and TSC datasets include DistalPhalanxTW, MiddlePhalanxTW and ProximalPhalanx (Ismail Fawaz et al., 2019a). We use MLP-Mixer (Tolstikhin et al., 2021), MLP and LSTM (Hochreiter & Schmidhuber, 1997) as the pretrained model. Our experiments are conducted on the clean trainsets, following the common setting of certified adversarial defenses (Yoon et al., 2022; Li et al., 2020; Cohen et al., 2019; Chiang et al., 2020; Zhang et al., 2019). Unless otherwise specified, We use MLP-Mixer as the base model for MIA, DS and RA, and $\Delta = 1.5$. The experiments are conducted on CPU (16 Intel(R) Xeon(R) Gold 5222 CPU @ 3.80GHz) and GPU (one NVIDIA RTX 2080 Ti). More details are omitted to Appendix.

Evaluation metrics. For TSC, we evaluate the defense by *certified accuracy* (CA) under the temporally-localized perturbation, which is defined by the fraction of the test samples that are correctly classified and certifiably robust to the perturbation. For TSC, we evaluate the defense by: *forecasting rate* (FR), *mean square error* (MSE) and *mean absolute error* (MAE)[4]. FR is the fraction of the test samples on which MIA outputs the forecast instead of **Abstain**. MSE/MAE measures the mean square error/mean absolute error between MIA forecasts (**Abstain** are excluded) and groundtruth. We omit the evaluation on multivariate tasks to Appendix due to space limitations.[5]

5.1 Comparison to Peer Methods

Comparison on TSC. Table 1 reports the certified accuracy of three methods in defending temporally-localized perturbations. The pretrained/base model architectures of three defenses are all

[4]We omit the evaluation of MAE to Appendix.

[5]In our experiments, $L_{\text{mask}} = c\%$ or $L_{\text{adv}} = c\%$ or $\eta = c\%$ refer to $c\% \cdot t_0$.

Table 2: (Exchange) Comparison among three certified defenses on TSF dataset.

Metric	Defense	1 %	2 %	3 %	4 %	5 %	6 %	7 %	8 %	9 %	10 %
FR (%)	MIA ($L_{\text{mask}} = 10\%$)	**82.2**	**82.2**	**83.2**	**82.2**	**82.2**	**81.2**	**81.2**	**81.2**	**80.2**	**79.2**
	DS ($\eta = 10\%$)	24.8	24.8	24.8	24.8	24.8	24.8	24.8	24.8	24.8	24.8
	RA ($\eta = 10\%$)	16.8	16.8	16.8	16.8	16.8	16.8	16.8	16.8	16.8	16.8
	MIA ($L_{\text{mask}} = 15\%$)	**64.4**	**71.3**	**69.3**	**69.3**	**71.3**	**68.3**	**69.3**	**71.3**	**62.4**	**65.3**
	DS ($\eta = 15\%$)	20.8	20.8	20.8	14.9	14.9	11.9	11.9	11.9	11.9	10.9
	RA ($\eta = 15\%$)	23.8	23.8	23.8	23.8	23.8	23.8	23.8	23.8	23.8	23.8
MSE	MIA ($L_{\text{mask}} = 10\%$)	**0.143**	**0.141**	**0.145**	**0.141**	**0.141**	**0.139**	**0.137**	**0.137**	**0.135**	**0.134**
	DS ($\eta = 10\%$)	0.192	0.192	0.192	0.192	0.192	0.192	0.192	0.192	0.192	0.192
	RA ($\eta = 10\%$)	0.202	0.202	0.202	0.202	0.202	0.202	0.202	0.202	0.202	0.202
	MIA ($L_{\text{mask}} = 15\%$)	**0.126**	**0.134**	**0.130**	0.132	0.137	0.132	0.129	0.130	0.123	0.125
	DS ($\eta = 15\%$)	0.144	0.144	0.144	**0.065**	**0.065**	**0.069**	**0.069**	**0.069**	**0.069**	**0.060**
	RA ($\eta = 15\%$)	0.248	0.248	0.248	0.248	0.248	0.248	0.248	0.248	0.248	0.248

Table 3: Comparison of the inference time (millisecond) of three defenses on TSC datasets.

Defense \ Model	FCN			MLP-Mixer			MLP			ResNet-18		
	2%	5%	10%	2%	5%	10%	2%	5%	10%	2%	5%	10%
MIA ($L_{\text{mask}} = 10\%$)	2.0	2.0	3.0	2.7	2.7	4.6	1.7	1.7	2.7	3.8	3.8	5.3
DS ($\eta = 10\%$)	0.6	0.6	0.6	2.0	2.0	2.0	0.3	0.3	0.3	2.6	2.6	2.6
RA ($\eta = 10\%$)	25.2	25.2	25.2	259.7	259.7	259.7	0.8	0.8	0.8	130.3	130.3	130.3
MIA ($L_{\text{mask}} = 15\%$)	2.0	2.0	2.0	2.7	2.7	2.7	1.7	1.7	1.7	3.8	3.8	3.8
DS ($\eta = 15\%$)	0.6	0.6	0.6	1.9	1.9	1.9	0.3	0.3	0.3	2.6	2.6	2.6
RA ($\eta = 15\%$)	25.3	25.3	25.3	260.6	260.6	260.6	0.8	0.8	0.8	130.4	130.4	130.4

Table 4: (Traffic) The performance of MIA on different pretrained models. (c_1 $c_2\%$) reports (MSE, FR%) of MIA. **Baseline** is MSE of the pretrained model without MIA. The lowest MSE and the highest FR for each pretrained model is shown in bold-face.

Model	Baseline	L_{mask}	$\Delta = 1.0$ 2%	5%	10%	$\Delta = 1.2$ 2%	5%	10%	$\Delta = 1.5$ 2%	5%	10%
MLP-Mixer	0.224	2%	**0.065** 72.3%			**0.072** 77.2%			0.144 89.1%		
		5%	0.067 75.2%	**0.068** 73.3%		0.079 **80.2%**	**0.075** 78.2%		**0.141** 90.1%	0.143 89.1%	
		10%	0.068 **77.2%**	0.069 **76.2%**	**0.066** **69.3%**	0.079 **80.2%**	0.079 **80.2%**	**0.075** **76.2%**	0.143 **91.1%**	**0.141** **90.1%**	**0.139** **88.1%**
GRU	0.243	2%	**0.067** 66.3%			**0.070** 73.3%			**0.143** 89.1%		
		5%	0.072 72.3%	**0.070** 68.3%		0.075 76.2%	**0.073** 74.3%		0.145 **91.1%**	**0.141** 88.1%	
		10%	0.070 **74.3%**	0.071 **72.3%**	**0.069** **63.4%**	0.074 **77.2%**	0.074 **77.2%**	**0.066** **70.3%**	0.145 **91.1%**	0.143 **90.1%**	**0.137** **86.1%**
LSTM	0.229	2%	**0.068** **66.3%**			**0.071** 76.2%			0.152 **91.1%**		
		5%	0.069 **66.3%**	**0.070** 65.3%		0.073 **77.2%**	**0.071** 76.2%		**0.149** 89.1%	**0.147** 88.1%	
		10%	0.070 65.3%	0.071 **66.3%**	**0.066** **61.4%**	0.073 **77.2%**	0.073 **77.2%**	**0.064** **72.3%**	0.150 89.1%	0.153 **90.1%**	**0.149** **87.1%**
MLP	0.222	2%	**0.064** 67.3%			**0.064** **72.3%**			0.148 90.1%		
		5%	0.067 **71.3%**	**0.064** 68.3%		**0.064** **72.3%**	**0.064** **72.3%**		0.148 **92.1%**	0.148 90.1%	
		10%	0.067 70.3%	0.067 **70.3%**	**0.063** **66.3%**	**0.064** **72.3%**	**0.064** **72.3%**	**0.063** **70.3%**	**0.146** 91.1%	**0.146** **91.1%**	**0.144** **89.1%**
ResNet18	0.248	2%	**0.074** 64.4%			0.087 75.2%			**0.149** 88.1%		
		5%	0.077 **68.3%**	**0.077** 65.3%		0.088 **79.2%**	0.089 **76.2%**		0.150 **89.1%**	**0.146** **87.1%**	
		10%	0.077 67.3%	0.078 **67.3%**	**0.076** **60.4%**	**0.086** 76.2%	**0.086** **76.2%**	**0.083** **73.3%**	0.150 88.1%	0.149 86.1%	**0.145** **83.2%**

MLP-Mixer. An interesting observation is that the certified accuracy of DS and RA keeps constant to different L_{adv}. The reason is that, the probability score of DS/RA models often concentrates on a single class, causing most classifications (including both (correct and wrong classifications) of DS and RA are of high robustness. The results show that the certified accuracy of MIA is more than twice of DR and RA across different L_{adv}. The reason is that the pretrained model of MIA classifies the masked series, while the base model in RS/DS classifies the subseries. MIA can attain a higher certified accuracy because the masked series contains much more information ($t_0 - L_{\text{mask}}$ unmasked time points) than the subseries (η sampled time points).

Comparison on TSF. Table 2 reports FR and MSE of three defenses on Exchange, where the model predicts the next 30 values. Here we utilize discretization technique to make the TSF task feasible to DS and RA. The table shows that MIA offers a significantly higher FR than DS and RA, implying that MIA return the forecasting results much more frequently than other two defenses. The reason for the superior FR is same as TSC. We also observe that DS ($\eta = 15\%$) achieves a lower MSE than MIA at $L_{\text{adv}} \geq 4\%$, which partially owing to its low FR. Since a low FR implies that the aggregation step of MIA filters a large portion of distrustful forecasts, reducing the difficulty of achieving lower MSE for the remained forecasts. Based on the results, MIA is better than other two defenses when we jointly consider FR and MSE.

Table 5: (Electricity) (c_1 $c_2\%$) report (MSE $\mathrm{FR}\%$) of MIA on different pretrained models.

Model	Baseline	L_{mask}	$\Delta = 1.0$ 2%	$\Delta = 1.0$ 5%	$\Delta = 1.0$ 10%	$\Delta = 1.2$ 2%	$\Delta = 1.2$ 5%	$\Delta = 1.2$ 10%	$\Delta = 1.5$ 2%	$\Delta = 1.5$ 5%	$\Delta = 1.5$ 10%
MLP-Mixer	0.388	2%	**0.093** 66.3%			0.094 64.4%			0.136 77.2%		
		5%	0.095 **69.3%**	**0.093** **68.3%**		0.096 **67.3%**	0.094 **66.3%**		0.134 **78.2%**	0.134 **78.2%**	
		10%	0.095 67.3%	0.095 67.3%	**0.089** **55.4%**	**0.091** 64.4%	**0.091** 64.4%	**0.089** **59.4%**	**0.134** 77.2%	**0.134** 77.2%	**0.116** **66.3%**
GRU	0.420	2%	**0.099** 62.4%			0.086 60.4%			**0.135** 68.3%		
		5%	0.100 64.4%	0.101 **63.4%**		0.087 **62.4%**	**0.087** **62.4%**		0.139 **69.3%**	**0.139** **69.3%**	
		10%	0.102 **65.3%**	**0.099** 62.4%	**0.103** **49.5%**	**0.085** 61.4%	0.087 61.4%	**0.086** **53.5%**	0.139 **69.3%**	**0.139** **69.3%**	**0.120** **64.4%**
LSTM	0.438	2%	0.100 64.4%			**0.082** 52.5%			0.142 70.3%		
		5%	**0.100** **66.3%**	0.101 **65.3%**		0.092 55.4%	**0.092** **55.4%**		**0.140** **71.3%**	**0.142** **70.3%**	
		10%	**0.100** **66.3%**	**0.100** 64.4%	**0.110** **51.5%**	0.091 **56.4%**	**0.092** **55.4%**	**0.094** **48.5%**	**0.140** **71.3%**	0.142 **70.3%**	**0.119** **59.4%**
MLP	0.402	2%	0.106 73.3%			**0.082** 61.4%			0.136 74.3%		
		5%	0.108 **77.2%**	0.105 **75.2%**		0.087 **65.3%**	**0.085** **63.4%**		**0.131** **77.2%**	0.132 **76.2%**	
		10%	**0.105** 75.2%	**0.105** **75.2%**	**0.098** **60.4%**	0.087 61.4%	0.087 61.4%	**0.084** **55.4%**	**0.131** **77.2%**	**0.126** **76.2%**	**0.108** **66.3%**
ResNet18	0.554	2%	0.093 51.5%			0.080 59.4%			**0.136** 66.3%		
		5%	**0.089** 51.5%	**0.089** 50.5%		0.080 **60.4%**	**0.080** **60.4%**		0.140 **68.3%**	0.140 **68.3%**	
		10%	0.094 **52.5%**	0.093 **51.5%**	**0.092** **43.6%**	**0.079** 56.4%	0.081 58.4%	**0.076** **54.5%**	0.141 67.3%	**0.136** 66.3%	**0.121** **61.4%**

Table 6: Comparison of different training algorithms on 3 TSC datasets.

Model	Training	L_{mask}	DistalPhalanxTW 5%	DistalPhalanxTW 10%	DistalPhalanxTW 15%	MiddlePhalanxTW 5%	MiddlePhalanxTW 10%	MiddlePhalanxTW 15%	ProximalPhalanxTW 5%	ProximalPhalanxTW 10%	ProximalPhalanxTW 15%
MLP-Mixer	Random	5%	62.4%			52.5%			65.3%		
		10%	61.4%	58.4%		53.5%	50.5%		73.3%	71.3%	
		15%	59.4%	59.4%	58.4%	59.4%	54.5%	49.5%	68.3%	67.3%	61.4%
	Masked	5%	**65.3%**			**64.4%**			**72.3%**		
		10%	**66.3%**	**63.4%**		**67.3%**	**60.4%**		**76.2%**	**74.3%**	
		15%	**64.4%**	**64.4%**	**60.4%**	**66.3%**	**62.4%**	**59.4%**	**76.2%**	**75.2%**	**74.3%**
FCN	Random	5%	63.4%			53.5%			68.3%		
		10%	66.3%	63.4%		52.5%	52.5%		70.3%	67.3%	
		15%	66.3%	65.3%	65.3%	57.4%	57.4%	56.4%	66.3%	66.3%	65.3%
	Masked	5%	**70.3%**			**64.4%**			**75.2%**		
		10%	**70.3%**	**69.3%**		**66.3%**	**65.3%**		**73.3%**	**71.3%**	
		15%	**70.3%**	**67.3%**	**66.3%**	**65.3%**	**63.4%**	**63.4%**	**75.2%**	**73.3%**	**73.3%**
MLP	Random	5%	62.4%			65.3%			72.3%		
		10%	62.4%	60.4%		59.4%	54.5%		76.2%	73.3%	
		15%	63.4%	61.4%	61.4%	61.4%	55.4%	55.4%	71.3%	71.3%	68.3%
	Masked	5%	**64.4%**			**69.3%**			**79.2%**		
		10%	**65.3%**	**64.4%**		**70.3%**	**67.3%**		**79.2%**	**78.2%**	
		15%	**66.3%**	**63.4%**	**63.4%**	**69.3%**	**66.3%**	**66.3%**	**78.2%**	**78.2%**	**77.2%**
ResNet-18	Random	5%	61.4%			57.4%			65.3%		
		10%	59.4%	57.4%		57.4%	56.4%		74.3%	67.3%	
		15%	58.4%	56.4%	55.4%	58.4%	58.4%	58.4%	74.3%	73.3%	66.3%
	Masked	5%	**65.3%**			**67.3%**			**78.2%**		
		10%	**66.3%**	**64.4%**		**63.4%**	**63.4%**		**78.2%**	**76.2%**	
		15%	**64.4%**	**61.4%**	**59.4%**	**65.3%**	**62.4%**	**62.4%**	**78.2%**	**78.2%**	**78.2%**

Comparison on inference time. Table 3 compares the inference time of three defenses, which is averaged among three TSC datasets. We observe that the inference time of MIA is larger than DS, but significantly smaller than RA. Specifically, MIA's larger inference time than DS is owing to the cost in running the imputation model. RA's large inference time is for the confidence interval estimation[6]. We also observe that the inference time of MIA increases with L_{adv}, and decreases with L_{mask}, because the number of masked series is $\lceil (t_0 - L_{mask})/(L_{\text{mask}} - L_{\text{adv}} + 1) \rceil + 1$. We omit the inference time analysis on TSF datasets to Appendix.

5.2 Analysis of MIA on Different Pretrained Models

Table 4 and Table 5 report the performance of MIA on different pretrained models, where the model forecasts the next 24 points. We observe that MIA ($\Delta = 1.0, 1.5$) consistently lowers MSE as compared to that of the original pretrained models, suggesting MIA could also be an effective plugin for performance improvement. Specifically, MIA improves the forecasting performance in the way of filtering these distrustful forecasts, sacrificing the availability (the decrease of FR) for lower MSE as well as certified robustness, which is a common trade-off in the field of certified defenses (Cohen et al., 2019; Levine & Feizi, 2020a;b; Liu et al., 2021; Han et al., 2021). We can control the trade-off between MSE and FR by Δ, as the decrease of Δ can reduce MSE and FR.

5.3 Analysis on Imputation Model of MIA and Ablation Study

Impact of training algorithm. Table 6 compares our masked training to random training, which trains the imputation model on the randomly masked series. Through extensive comparisons on different imputation model architectures and datasets, we convince that masked training consistently

[6]Following the official implementation of RA (Levine & Feizi, 2020b), we take $100,000$ samples for the confidence interval estimation.

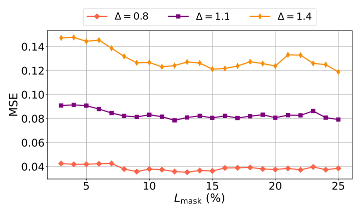

(a) MSE v.s L_{mask}

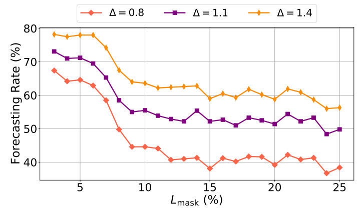

(b) FR v.s L_{mask}

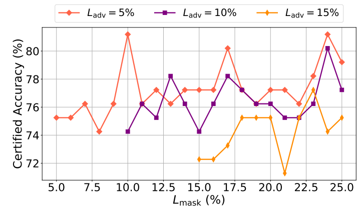

(c) CA v.s L_{mask}

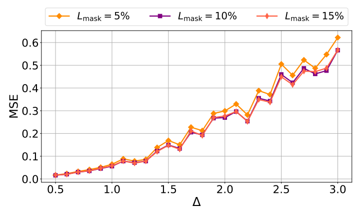

(d) MSE v.s Δ

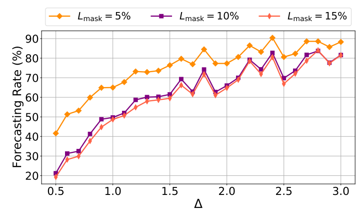

(e) FR v.s Δ

Figure 2: **Top**: impact of L_{mask} on TSC dataset ProximalPhalanxTW. **Bottom**: impact of Δ on TSF dataset Traffic ($L_{\text{adv}} = 3\%$).

Table 7: Comparison of four imputation models. The best results are shown in bold-face.

Model	L_{mask}	Electricity			Exchange			Traffic		
		2%	5%	10%	2%	5%	10%	2%	5%	10%
MLP-Mixer	2%	0.136 **77.2%**			0.158 **87.1%**			0.144 **89.1%**		
	5%	0.134 **78.2%**	0.134 **78.2%**		0.144 **83.2%**	0.138 **81.2%**		0.141 **90.1%**	0.143 **89.1%**	
	10%	0.134 **77.2%**	0.134 **77.2%**	0.116 **66.3%**	0.141 **82.2%**	0.141 **82.2%**	0.134 **79.2%**	0.143 **91.1%**	0.141 **90.1%**	0.139 **88.1%**
BRITS	2%	0.118 65.3%			0.118 40.6%			0.142 87.1%		
	5%	0.110 71.3%	0.099 59.4%		0.118 49.5%	0.098 15.8%		0.136 84.2%	0.130 75.2%	
	10%	0.099 61.4%	0.100 60.4%	0.094 45.5%	0.207 10.9%	0.277 1.0%	0.000 0.0%	0.128 79.2%	0.129 77.2%	0.123 73.3%
SAITS	2%	0.101 58.4%			**0.095** 25.7%			**0.120** 67.3%		
	5%	**0.091** 53.5%	**0.090** 52.5%		0.137 43.6%	0.101 27.7%		0.128 73.3%	**0.121** 68.3%	
	10%	0.104 56.4%	0.103 54.5%	0.094 44.6%	0.070 7.9%	0.048 6.9%	**0.001** 4.0%	0.125 67.3%	0.132 69.3%	0.124 59.4%
Transformer	2%	**0.085** 52.5%			0.145 23.8%			0.130 68.3%		
	5%	0.110 52.5%	0.113 42.6%		**0.072** 6.9%	**0.001** 2.0%		**0.127** 74.3%	0.123 65.3%	
	10%	**0.096** 60.4%	**0.093** 58.4%	**0.093** 34.7%	**0.029** 8.9%	**0.036** 7.9%	0.001 5.0%	**0.124** 75.2%	**0.127** 74.3%	**0.123** 61.4%

outperforms random training for MIA by a non-trivial gap. The gap becomes even larger at larger L_{adv}. The results suggest that masked training is suitable for MIA imputation model.

Impact of architecture of imputation models. Table 7 reports the performances of different imputation model architectures on MIA. Our results show that MLP-Mixer can offer higher FR and lower MSE simultaneously, suggesting MLP-Mixer is intrinsically more robust than other models.

Impact of L_{mask}. Fig. 2a, 2b show: 1) MSE roughly keeps constant w.r.t. L_{mask}, because the discretization technique can diminish the difference between the forecasts that are close to each other. 2) FR decreases with the increase of L_{mask}, because our imputation quality decreases with L_{mask}, making it harder to reach agreement unanimously. Fig. 2c show that the impact of L_{mask} on CA is not significant. Although the increase of L_{mask} reduces our imputation quality, it reduces the number of masked series simultaneously.

Impact of Δ. Fig. 2d, 2e report the impact of Δ. As Δ increases, we observe that MSE and FR increase, validating our statement about Δ in Section 4.1.

6 Conclusion

In this paper, we propose the first framework for time-series models to certifiably defend against ℓ_0-norm perturbations. Notably, MIA is a plug-and-play defense, which can be easily applied to any TSF/TSC pretrained model. The only requirement of deploying MIA is to train an imputation model, which has been extensively explored in this work. Moreover, our extensive experiments validate the effectiveness of MIA. We expect our work can inspire more studies on the ℓ_0-norm robustness for time-series models. Interesting future works include applying MIA to probabilistic models.

References

Alexander Alexandrov, Konstantinos Benidis, Michael Bohlke-Schneider, Valentin Flunkert, Jan Gasthaus, Tim Januschowski, Danielle C Maddix, Syama Rangapuram, David Salinas, Jasper Schulz, et al. Gluonts: Probabilistic time series models in python. *arXiv preprint arXiv:1906.05264*, 2019.

Anish Athalye and Nicholas Carlini. On the robustness of the cvpr 2018 white-box adversarial example defenses. *arXiv preprint arXiv:1804.03286*, 2018.

Anish Athalye, Nicholas Carlini, and David Wagner. Obfuscated gradients give a false sense of security: Circumventing defenses to adversarial examples. In *ICML*, 2018.

Wei Cao, Dong Wang, Jian Li, Hao Zhou, Lei Li, and Yitan Li. Brits: Bidirectional recurrent imputation for time series. In *NeurIPS*, 2018.

Nicholas Carlini and David Wagner. Adversarial examples are not easily detected: Bypassing ten detection methods. In *Proceedings of the 10th ACM workshop on artificial intelligence and security*, pp. 3–14, 2017.

Ping-yeh Chiang, Michael Curry, Ahmed Abdelkader, Aounon Kumar, John Dickerson, and Tom Goldstein. Detection as regression: Certified object detection with median smoothing. In *NeurIPS*, 2020.

Kyunghyun Cho, Bart van Merrienboer, Çaglar Gülçehre, Dzmitry Bahdanau, Fethi Bougares, Holger Schwenk, and Yoshua Bengio. Learning phrase representations using RNN encoder-decoder for statistical machine translation. In *EMNLP*, 2014.

Moustapha Cisse, Piotr Bojanowski, Edouard Grave, Yann Dauphin, and Nicolas Usunier. Parseval networks: Improving robustness to adversarial examples. In *ICML*, 2017.

Charles J Clopper and Egon S Pearson. The use of confidence or fiducial limits illustrated in the case of the binomial. *Biometrika*, 1934.

Jeremy M. Cohen, Elan Rosenfeld, and J. Zico Kolter. Certified adversarial robustness via randomized smoothing. In *ICML*, 2019.

Jerome T Connor, R Douglas Martin, and Les E Atlas. Recurrent neural networks and robust time series prediction. *IEEE transactions on neural networks*, 1994.

Raphaël Dang-Nhu, Gagandeep Singh, Pavol Bielik, and Martin Vechev. Adversarial attacks on probabilistic autoregressive forecasting models. In *ICML*, 2020.

Emmanuel de Bézenac, Syama Sundar Rangapuram, Konstantinos Benidis, Michael Bohlke-Schneider, Richard Kurle, Lorenzo Stella, Hilaf Hasson, Patrick Gallinari, and Tim Januschowski. Normalizing kalman filters for multivariate time series analysis. In *Neural Information Processing Systems*, 2020.

Ailin Deng and Bryan Hooi. Graph neural network-based anomaly detection in multivariate time series. *AAAI*, 2021.

Daizong Ding, Mi Zhang, Yuanmin Huang, Xudong Pan, Fuli Feng, Erling Jiang, and Min Yang. Towards backdoor attack on deep learning based time series classification. In *2022 IEEE 38th International Conference on Data Engineering (ICDE)*, pp. 1274–1287. IEEE, 2022.

Wenjie Du, David Côté, and Yan Liu. Saits: Self-attention-based imputation for time series. *arXiv preprint arXiv:2202.08516*, 2022.

Hassan Ismail Fawaz, Germain Forestier, Jonathan Weber, Lhassane Idoumghar, and Pierre-Alain Muller. Adversarial attacks on deep neural networks for time series classification. In *IJCNN*, 2019.

Vincent Fortuin, Dmitry Baranchuk, Gunnar Rätsch, and Stephan Mandt. Gp-vae: Deep probabilistic time series imputation. In *International conference on artificial intelligence and statistics*, 2020.

WR Foster, F Collopy, and LH Ungar. Neural network forecasting of short, noisy time series. *Computers & chemical engineering*, 1992.

Sarah Gelper, Roland Fried, and Christophe Croux. Robust forecasting with exponential and holt–winters smoothing. *Journal of forecasting*, 2010.

Tian Guo, Zhao Xu, Xin Yao, Haifeng Chen, Karl Aberer, and Koichi Funaya. Robust online time series prediction with recurrent neural networks. In *DSAA*. Ieee, 2016.

Husheng Han, Kaidi Xu, Xing Hu, Xiaobing Chen, Ling Liang, Zidong Du, Qi Guo, Yanzhi Wang, and Yunji Chen. Scalecert: Scalable certified defense against adversarial patches with sparse superficial layers. In *NeurIPS*, 2021.

Xintian Han, Yuxuan Hu, Luca Foschini, Larry Chinitz, Lior Jankelson, and Rajesh Ranganath. Deep learning models for electrocardiograms are susceptible to adversarial attack. *Nature medicine*, 2020.

Kaiming He, Xiangyu Zhang, Shaoqing Ren, and Jian Sun. Deep residual learning for image recognition. In *CVPR*, 2016.

Dan Hendrycks and Kevin Gimpel. Gaussian error linear units (gelus). *arXiv preprint arXiv:1606.08415*, 2016.

Sepp Hochreiter and Jürgen Schmidhuber. Long short-term memory. *Neural computation*, 9(8): 1735–1780, 1997.

Kyle Hundman, Valentino Constantinou, Christopher Laporte, Ian Colwell, and Tom Söderström. Detecting spacecraft anomalies using lstms and nonparametric dynamic thresholding. *KDD*, 2018.

Jeng-Ren Hwang, Shyi-Ming Chen, and Chia-Hoang Lee. Handling forecasting problems using fuzzy time series. *Fuzzy sets and systems*, 1998.

Hassan Ismail Fawaz, Germain Forestier, Jonathan Weber, Lhassane Idoumghar, and Pierre-Alain Muller. Deep learning for time series classification: a review. *Data Mining and Knowledge Discovery*, 33(4):917–963, 2019a.

Hassan Ismail Fawaz, Germain Forestier, Jonathan Weber, Lhassane Idoumghar, and Pierre-Alain Muller. Deep learning for time series classification: a review. *Data mining and knowledge discovery*, 2019b.

Fazle Karim, Somshubra Majumdar, and Houshang Darabi. Adversarial attacks on time series. *PAMI*, 2020.

J. Ke, H. Zheng, H. Yang, and X. M. Chen. Short-term forecasting of passenger demand under on-demand ride services: A spatio-temporal deep learning approach. *Transportation research part C: Emerging technologies*, 2017.

Diederik P. Kingma and Jimmy Ba. Adam: A method for stochastic optimization, 2014.

Alexander Levine and Soheil Feizi. (de) randomized smoothing for certifiable defense against patch attacks. In *NeurIPS*, 2020a.

Alexander Levine and Soheil Feizi. Robustness certificates for sparse adversarial attacks by randomized ablation. In *AAAI*, 2020b.

Dan Li, Dacheng Chen, Lei Shi, Baihong Jin, Jonathan Goh, and See-Kiong Ng. Mad-gan: Multivariate anomaly detection for time series data with generative adversarial networks. In *ICANN*, 2019.

Hui Li, Yunpeng Cui, Shuo Wang, Juan Liu, Jinyuan Qin, and Yilin Yang. Multivariate financial time-series prediction with certified robustness. *IEEE Access*, 2020.

Zhihan Li, Youjian Zhao, Jiaqi Han, Ya Su, Rui Jiao, Xidao Wen, and Dan Pei. Multivariate time series anomaly detection and interpretation using hierarchical inter-metric and temporal embedding. *KDD*, 2021.

Hongbin Liu, Jinyuan Jia, and Neil Zhenqiang Gong. Pointguard: Provably robust 3d point cloud classification. In *CVPR*, 2021.

Yonghong Luo, Ying Zhang, Xiangrui Cai, and Xiaojie Yuan. E2gan: End-to-end generative adversarial network for multivariate time series imputation. In *Proceedings of the 28th international joint conference on artificial intelligence*, 2019.

Michael McCoyd, Won Park, Steven Chen, Neil Shah, Ryan Roggenkemper, Minjune Hwang, Jason Xinyu Liu, and David Wagner. Minority reports defense: Defending against adversarial patches. In *International Conference on Applied Cryptography and Network Security*, 2020.

Takeru Miyato, Andrew M Dai, and Ian Goodfellow. Adversarial training methods for semi-supervised text classification. In *ICLR*, 2017.

Steffen Moritz and Thomas Bartz-Beielstein. imputets: time series missing value imputation in r. *R J.*, pp. 207, 2017.

Izaskun Oregi, Javier Del Ser, Aritz Perez, and Jose A Lozano. Adversarial sample crafting for time series classification with elastic similarity measures. In *International Symposium on Intelligent and Distributed Computing*, pp. 26–39. Springer, 2018.

Daehyung Park, Yuuna Hoshi, and Charles C. Kemp. A multimodal anomaly detector for robot-assisted feeding using an lstm-based variational autoencoder. *RA-L*, 2018.

Nikolaos Passalis, Manos Kirtas, George Mourgias-Alexandris, George Dabos, Nikos Pleros, and Anastasios Tefas. Training noise-resilient recurrent photonic networks for financial time series analysis. In *2020 28th European Signal Processing Conference (EUSIPCO)*, 2021.

Joseph D Piotroski. Value investing: The use of historical financial statement information to separate winners from losers. *Journal of Accounting Research*, pp. 1–41, 2000.

Lukas Ruff, Nico Görnitz, Lucas Deecke, Shoaib Ahmed Siddiqui, Robert A. Vandermeulen, Alexander Binder, Emmanuel Müller, and M. Kloft. Deep one-class classification. In *ICML*, 2018.

David Salinas, Michael Bohlke-Schneider, Laurent Callot, Roberto Medico, and Jan Gasthaus. High-dimensional multivariate forecasting with low-rank gaussian copula processes. *NeurIPS*, 2019.

David Salinas, Valentin Flunkert, Jan Gasthaus, and Tim Januschowski. Deepar: Probabilistic forecasting with autoregressive recurrent networks. *International Journal of Forecasting*, pp. 1181–1191, 2020.

Hadi Salman, Mingjie Sun, Greg Yang, Ashish Kapoor, and J Zico Kolter. Denoised smoothing: A provable defense for pretrained classifiers. In *NeurIPS*, 2020.

T. Schlegl, Philipp Seeböck, S. Waldstein, G. Langs, and U. Schmidt-Erfurth. f-anogan: Fast unsupervised anomaly detection with generative adversarial networks. *Med. Image Anal.*, 2019.

B. Schölkopf, John C. Platt, J. Shawe-Taylor, Alex Smola, and R. C. Williamson. Estimating the support of a high-dimensional distribution. *Neural Comput.*, 2001.

Shahroz Tariq, Sangyup Lee, Youjin Shin, Myeong Shin Lee, Okchul Jung, Daewon Chung, and Simon S. Woo. Detecting anomalies in space using multivariate convolutional lstm with mixtures of probabilistic pca. *KDD*, 2019.

D. Tax and R. Duin. Support vector data description. *Mach. Learn.*, 2004.

Ilya O Tolstikhin, Neil Houlsby, Alexander Kolesnikov, Lucas Beyer, Xiaohua Zhai, Thomas Unterthiner, Jessica Yung, Andreas Steiner, Daniel Keysers, Jakob Uszkoreit, et al. Mlp-mixer: An all-mlp architecture for vision. In *NeurIPS*, 2021.

Ashish Vaswani, Noam Shazeer, Niki Parmar, Jakob Uszkoreit, Llion Jones, Aidan N Gomez, Lukasz Kaiser, and Illia Polosukhin. Attention is all you need. In *NeurIPS*, 2017.

Eric Wong and J Zico Kolter. Provable defenses against adversarial examples via the convex outer adversarial polytope. In *ICML*, 2018.

Haixu Wu, Jiehui Xu, Jianmin Wang, and Mingsheng Long. Autoformer: Decomposition transformers with Auto-Correlation for long-term series forecasting. In *NeurIPS*, 2021.

Chong Xiang and Prateek Mittal. Patchguard++: Efficient provable attack detection against adversarial patches. *arXiv*, 2021.

Chong Xiang, Arjun Nitin Bhagoji, Vikash Sehwag, and Prateek Mittal. {PatchGuard}: A provably robust defense against adversarial patches via small receptive fields and masking. In *30th USENIX Security Symposium (USENIX Security 21)*, pp. 2237–2254, 2021.

Chong Xiang, Saeed Mahloujifar, and Prateek Mittal. {PatchCleanser}: Certifiably robust defense against adversarial patches for any image classifier. In *31st USENIX Security Symposium (USENIX Security 22)*, pp. 2065–2082, 2022.

Haowen Xu, Wenxiao Chen, N. Zhao, Zeyan Li, Jiahao Bu, Zhihan Li, Y. Liu, Y. Zhao, Dan Pei, Yang Feng, Jian Jhen Chen, Zhaogang Wang, and Honglin Qiao. Unsupervised anomaly detection via variational auto-encoder for seasonal kpis in web applications. *WWW*, 2018.

Jiehui Xu, Haixu Wu, Jianmin Wang, and Mingsheng Long. Anomaly transformer: Time series anomaly detection with association discrepancy. In *ICLR*, 2022.

Takehisa Yairi, Naoya Takeishi, Tetsuo Oda, Yuta Nakajima, Naoki Nishimura, and Noboru Takata. A data-driven health monitoring method for satellite housekeeping data based on probabilistic clustering and dimensionality reduction. *IEEE Trans. Aerosp. Electron. Syst.*, 2017.

Bo Yang, Xiao Fu, Nicholas D Sidiropoulos, and Mingyi Hong. Towards k-means-friendly spaces: Simultaneous deep learning and clustering. In *ICML*, 2017.

Wenbo Yang, Jidong Yuan, Xiaokang Wang, and Peixiang Zhao. Tsadv: Black-box adversarial attack on time series with local perturbations. *Engineering Applications of Artificial Intelligence*, 114: 105218, 2022.

Yun Yang and ChongJun Fan. Efficient and robust time series prediction model based on remd-mmlp with temporal-window. *Expert Systems with Applications*, 2022.

Zhongguo Yang, Han Li, Mingzhu Zhang, Jingbin Wang, and Chen Liu. A method for resisting adversarial attack on time series classification model in iot system. In *International Conference on Web Information Systems and Applications*, pp. 559–566. Springer, 2020.

TaeHo Yoon, Youngsuk Park, Ernest K Ryu, and Yuyang Wang. Robust probabilistic time series forecasting. In *AISTATS*, 2022.

Ceylan Yozgatligil, Sipan Aslan, Cem Iyigun, and Inci Batmaz. Comparison of missing value imputation methods in time series: the case of turkish meteorological data. *Theoretical and applied climatology*, 2013.

Huan Zhang, Hongge Chen, Chaowei Xiao, Bo Li, Duane Boning, and Cho-Jui Hsieh. Towards stable and efficient training of verifiably robust neural networks. *arXiv preprint arXiv:1906.06316*, 2019.

Zhanyuan Zhang, Benson Yuan, Michael McCoyd, and David Wagner. Clipped bagnet: Defending against sticker attacks with clipped bag-of-features. In *2020 IEEE Security and Privacy Workshops (SPW)*, pp. 55–61. IEEE, 2020.

Hang Zhao, Yujing Wang, Juanyong Duan, Congrui Huang, Defu Cao, Yunhai Tong, Bixiong Xu, Jing Bai, Jie Tong, and Qi Zhang. Multivariate time-series anomaly detection via graph attention network. *ICDM*, 2020.

Bin Zhou, Shenghua Liu, Bryan Hooi, Xueqi Cheng, and Jing Ye. Beatgan: Anomalous rhythm detection using adversarially generated time series. In *IJCAI*, 2019.

Haoyi Zhou, Shanghang Zhang, Jieqi Peng, Shuai Zhang, Jianxin Li, Hui Xiong, and Wancai Zhang. Informer: Beyond efficient transformer for long sequence time-series forecasting. In *AAAI*, 2021.

A Proof for Proposition 1

Proposition 2 (Robustness Certificate of MIA)**.** The forecast/label (not **Abstain**) returned by Algorithm 1 cannot be changed by any temporally-localized perturbation whose ℓ_0 norm is no larger than L_{adv} (see proof in Appendix).

Proof. Here we prove the robustness certificate for MIA (TSC). The proof for MIA (TSF) is analogous to this proof. Assume that the adversary has changed the classification result of MIA from y_1 to y_2 via the temporally-localized perturbation δ (ℓ_0 norm is L_{adv}). For notational simplicity we denote $\mathrm{M}_{[1+k\alpha:\min(L_{mask}+k\alpha,t_0)]}$ by $\mathrm{M}^{(k)}, k=0,\ldots,\lceil(t_0-L_{\text{mask}})/\alpha\rceil$ and denote $\boldsymbol{\delta}_{[t_{\text{adv}}+1:t_{\text{adv}}+L_{\text{adv}}]}$ by $\boldsymbol{\delta}^{(t_{\text{adv}})}, t_{\text{adv}}=0,\ldots,t_0-L_{\text{adv}}$. Then, we have:

$$f(\mathbf{x}_{1:t_0}\odot\mathrm{M}^{(0)})=f(\mathbf{x}_{1:t_0}\odot\mathrm{M}^{(1)})=\ldots=y_1 \tag{12}$$

$$f((\mathbf{x}_{1:t_0}+\boldsymbol{\delta}^{(t_{\text{adv}})})\odot\mathrm{M}^{(0)})=f((\mathbf{x}_{1:t_0}+\boldsymbol{\delta}^{(t_{\text{adv}})})\odot\mathrm{M}^{(1)})=\ldots=y_2 \tag{13}$$

Then our next step is to prove that *there exists a mask $M^{(\hat{m})}, \hat{m}\in\{0,\ldots,\lceil t_0-L_{\text{mask}})/\alpha\rceil\}$ that can occlude the perturbation*. Specifically, we show that the mask $\mathrm{M}^{(\lfloor\frac{t_{\text{adv}}}{\alpha}\rfloor)}$ can cover the perturbation. First, we show the presence of the mask $\mathrm{M}^{(\lfloor\frac{t_{\text{adv}}}{\alpha}\rfloor)}$ by proving $\lfloor\frac{t_{\text{adv}}}{\alpha}\rfloor\le\lceil(t_0-L_{\text{mask}})/\alpha\rceil$, as follow:

$$\frac{t_{\text{adv}}}{\alpha}-\frac{t_0-L_{\text{mask}}}{\alpha}\le\frac{t_0-L_{\text{adv}}-t_0+L_{\text{mask}}}{L_{\text{mask}}-L_{\text{adv}}+1}=\frac{L_{\text{mask}}-L_{\text{adv}}}{L_{\text{mask}}-L_{\text{adv}}+1}<1 \tag{14}$$

Second, we show that $\mathrm{M}^{(\lfloor\frac{t_{\text{adv}}}{\alpha}\rfloor)}$ covers the perturbation by comparing the starting/end point of the mask $\mathrm{M}^{(\frac{t_{\text{adv}}}{\alpha})}$ and the perturbation δ. For the starting point, we have:

$$\underbrace{(\alpha\lfloor\frac{t_{\text{adv}}}{\alpha}\rfloor+1)}_{\text{Mask}}-\underbrace{(t_{\text{adv}}+1)}_{\text{Perturbation}}\le 0 \tag{15}$$

In terms of the end points, we have:

$$\underbrace{(\alpha\lfloor\frac{t_{\text{adv}}}{\alpha}\rfloor+1+L_{\text{mask}})}_{\text{Mask}}-\underbrace{(t_{\text{adv}}+L_{\text{adv}})}_{\text{Perturbation}} \tag{16}$$

$$=\alpha\lfloor\frac{t_{\text{adv}}}{\alpha}\rfloor+(L_{\text{mask}}-L_{\text{adv}}+1)-t_{\text{adv}} \tag{17}$$

$$=\alpha(\lfloor\frac{t_{\text{adv}}}{\alpha}\rfloor+1)-t_{\text{adv}}\ge 0 \tag{18}$$

As $\mathrm{M}^{(\hat{m})}$ occludes the perturbation, thus $(\mathbf{x}_{1:t_0})\odot\mathrm{M}^{(\hat{m})}=(\mathbf{x}_{1:t_0}+\boldsymbol{\delta}^{(t_{\text{adv}})})\odot\mathrm{M}^{(\hat{m})}\Rightarrow y_1=y_2$. Our proof is completed.

B Empirical Evaluation on Risk of Temporally-Localized Perturbations

To support our statement about the risk of temporally-localized perturbations, we specifically propose an algorithm for generating the temporally-localized perturbations. We then evaluate the attack performance visually.

B.1 Restate Definition of temporally-localized Perturbation

Definition 2 (Temporally-localized perturbation)**.** Temporally-localized perturbation is to *perturb consecutive time points of* $\mathbf{x}_{1:t_0}$ *w.r.t. ℓ_0-norm constraint*. The perturbed series is:

$$\begin{aligned}&\mathbf{x}_{1:t_0}+\boldsymbol{\delta}_{[t_{\text{adv}}+1:t_{\text{adv}}+L_{\text{adv}}]}\quad\text{subject to}\quad\|\boldsymbol{\delta}_{[t_{\text{adv}}+1:t_{\text{adv}}+L_{\text{adv}}]}\|_0\le L_{\text{adv}}\\&=\mathbf{x}_{1:t_0}+[0,\ldots,\delta_{t_{\text{adv}}+1},\ldots,\delta_{t_{\text{adv}}+L_{\text{adv}}},0,\ldots,0]\\&=[x_1,\ldots,\underbrace{x_{t_{\text{adv}}+1}+\delta_{t_{\text{adv}}+1},\ \ldots,\ x_{t_{\text{adv}}+L_{\text{adv}}}+\delta_{t_{\text{adv}}+L_{\text{adv}}}}_{\text{Perturbed subsequence}},\ \ldots,x_{t_0}]\end{aligned} \tag{19}$$

where $t_{\text{adv}}+1$ and L_{adv} are the starting point and the ℓ_0-norm of the temporally-localized perturbation $\boldsymbol{\delta}_{[t_{\text{adv}}+1:t_{\text{adv}}+L_{\text{adv}}]}$.

Table 8: (Traffic) Evaluate MSE between the clean forecasts and the perturbed forecasts. The temporally-localized perturbations is generated subject to different ℓ_0-norm constraints ($L_{\text{adv}} = 2\%, 5\%, 10\%$) and ℓ_2-norm constraints $(1.0, 1.5, 2.0, 2.5, 3.0, 3.5)$.

Model	L_{adv}	1.0	1.5	2.0	2.5	3.0	3.5
MLP	2%	1.614	1.675	1.731	1.547	1.482	1.469
	5%	1.437	1.375	1.295	1.288	1.472	1.590
	10%	1.318	1.204	1.137	1.418	1.686	1.865
MLP-Mixer	2%	0.156	0.156	0.188	0.283	0.400	0.425
	5%	0.154	0.502	0.322	0.148	0.148	0.148
	10%	0.071	0.321	0.282	0.201	0.220	0.150
LSTM	2%	0.059	0.132	0.152	0.422	0.212	0.176
	5%	0.323	0.503	0.646	0.630	0.852	0.929
	10%	0.166	0.290	0.652	0.803	1.301	1.753

B.2 Algorithm of Generating Temporally-Localized Perturbations.

The objective of our algorithm is to maximize MSE between the original forecasts and the perturbed forecasts, with respect to the ℓ_0-norm constraint. Specifically, given the forecasting model $f(\mathbf{x}_{1:t_0}) \rightarrow \mathbf{x}_{t_0+1,t_0+\tau}$, our objective can be formulated as follows:

$$\arg\max_{\boldsymbol{\delta}} |f(\mathbf{x}_{1:t_0} + \boldsymbol{\delta}) - f(\mathbf{x}_{1:t_0})|_2^2 \tag{20}$$

where δ corresponds to the perturbation defined in Eq.(19). Actually, the problem of computing the temporally-localized perturbation can be decomposed into two sub-problems: **P1**) Search for the period $[t_{\text{adv}}+1, t_{\text{adv}}+L_{\text{adv}}]$ to perturb. **P2**) Fix the period $[t_{\text{adv}}+1, t_{\text{adv}}+L_{\text{adv}}]$, compute the value of the perturbation $\delta_{t_{\text{adv}}+1}, \ldots, \delta_{t_{\text{adv}}+L_{\text{adv}}}$. Here solving **P2** is not hard. If we have determined $\delta_{t_{\text{adv}}+1}, \ldots, \delta_{t_{\text{adv}}+L_{\text{adv}}}$, we can maximize the following loss to compute the perturbation values via projected gradient descent (PGD).

$$\max_{\delta_{t_{\text{adv}}+1},\ldots,\delta_{t_{\text{adv}}+L_{\text{adv}}}} |f(\mathbf{x}_{1:t_0} + \boldsymbol{\delta}) - f(\mathbf{x}_{1:t_0})|_2^2 \tag{21}$$

Then the main challenge is to determined which period to perturb. Here we solve **P1** by enumerating all the possible perturbing positions $[t_{\text{adv}}+1 : t_{\text{adv}}+L_{\text{adv}}],\ t_{\text{adv}} = 0, \ldots, t_0 - L_{\text{adv}}$ and compute the corresponding attacks. Finally, we return the one with the largest MSE loss among $t_0 - L_{\text{adv}} + 1$ perturbations. However, in practice we found that computing the values of perturbation (**P2**) w.r.t. to the fixed period is hard to converge, as the ℓ_2 norm of the temporally-localized perturbation will approach ∞. We believe that a perturbation attack with ∞ ℓ_2 norm is meaningless in practice. In the sake of practicality, we additionally consider ℓ_2 norm for the temporally-localized perturbations besides ℓ_0-norm constraint for the sub-problem **P2** , as follows:

$$\max_{\delta_{t_{\text{adv}}+1},\ldots,\delta_{t_{\text{adv}}+L_{\text{adv}}}} |f(\mathbf{x}_{1:t_0} + \boldsymbol{\delta}) - f(\mathbf{x}_{1:t_0})|_2^2 \text{subject to} \|\boldsymbol{\delta}\|_2^2 \leq \epsilon \tag{22}$$

where ϵ is the preset upper bound of the perturbation ℓ_2 norm.

B.3 Empirical Evaluation of Temporally-localized Perturbations.

B.4 Quantify the risk of temporally-localized perturbations.

Table 8 quantifies the risk of temporally-localized perturbations via computing MSE between the clean forecasts and the perturbed forecasts w.r.t. the ℓ_0-norm (L_{adv}) and the ℓ_2-norm (ϵ) constraints. We observe that MLP-Mixer model provides the highest empirical robustness among three models, which partially explains why MLP-Mixer outperforms other models on MIA. In particular, we further compare MLP to MLP+MIA ($\delta = 1.5$) in Table 4 of the main paper. Specifically, MSE of MLP under temporally-localized perturbations ($\epsilon = 3.0$) is $5\% : 1.472,\ 10\% : 0.1.686$ while MLP+MIA is $5\% : 0.146,\ 10\% : 0.144$. MIA reduces the MSE to roughly one tenth of the original, which indicates that MIA can effectively prevent our forecasting results from being influenced by the temporally-localized perturbations.

Table 9: Dataset information for TSF and TSC.

Dataset	Context length	Forecasting length	Number of classes
Electricity	96	24	N/A
Exchange	120	30	N/A
Traffic	96	24	N/A
DistalPhalanxTW	80	N/A	6
MiddlePhalanxTW	80	N/A	6
ProximalPhalanxTW	80	N/A	6

B.5 Compare Attacking Performance of ℓ_0 Attack to ℓ_2 Attack

We compare the ℓ_0 attack and ℓ_2 attack under under norm constraints β (attack rate) on time series forecasting task. Results are shown in Table 30, 31 and 32. The values in tables are calculated as $\frac{\text{MSE}_{\ell_0} - \text{MSE}_{\ell_2}}{\text{MSE}_{\ell_2}} \times 100\%$.

B.6 Visualize the risk of temporally-localized perturbations.

Fig. 3 illustratively shows the effect of temporally-localized perturbations on our forecasting results. We observe that temporally-localized perturbations of $L_{\text{atk}} = 10\%$ can significantly change our forecasts.

C Experimental Setups

C.1 Dataset Information

Table 9 shows the details of each dataset, including context length, forecasting length (for TSF datasets) and number of classes.

Traffic Hourly occupancy rate, between 0 and 1, of 963 San Francisco car lanes (Salinas et al., 2019).

Electricity Hourly time series of the electricity consumption of 370 customers (Salinas et al., 2019).

Exchange Daily exchange rate between 8 currencies (Salinas et al., 2019).

DistalPhalanxTW, MiddlePhalanxTW, ProximalPhalanxTw [7] This series of 11 classification problems were created as part of Luke Davis's PhD titled "Predictive Modelling of Bone Ageing". They are designed to test the efficacy of hand and bone outline detection and whether these outlines could be helpful in bone age prediction. Note that these problems are aligned by subject, and hence can be treated as a multi-dimensional TSC problem. The final three bone classification problems, DistalPhalanxTW, MiddlePhalanxTW and ProximalPhalanxTW, involve predicting the Tanner-Whitehouse score (as labelled by a human expert) from the outline.

Data Pre-Processing We pre-process the input series with *scipy.signal.savgol_filter* with window length 15 and polyorder 5 on both training and testing datasets. Besides, we normalize each input series with its mean value and standard deviation. Mean value and standard deviation will be 0 and 1 respectively for each normalized input series. We use the instance normalization method on both trainsets and testsets.

[7] `https://timeseriesclassification.com/description.php`

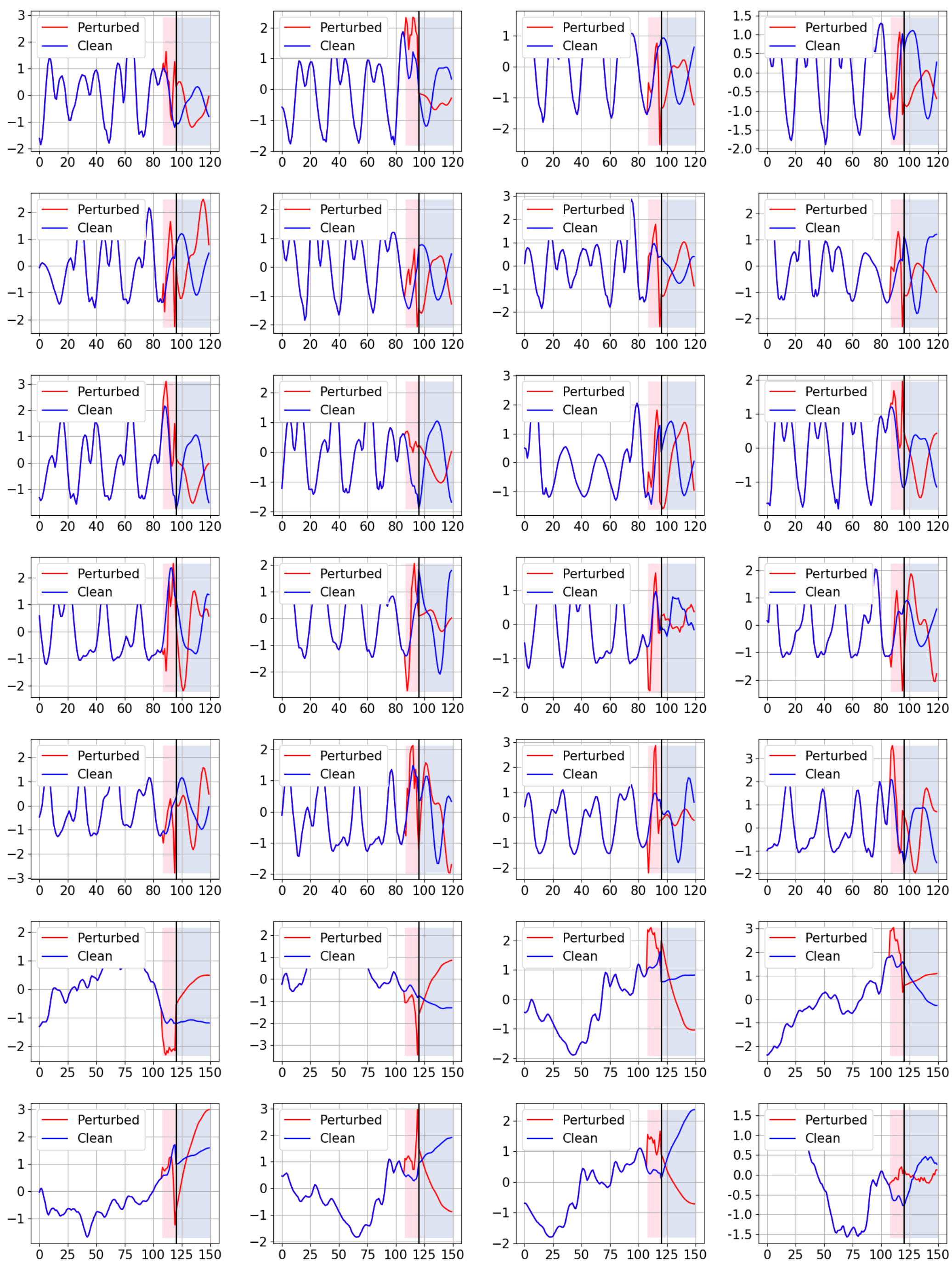

Figure 3: The effect of temporally-localized perturbations ($L_{\text{atk}} = 10\%$ and $\epsilon = 3.0$) on different datasets. Clean and Perturbed refer to the normal input series and the temporally-localized perturbations respectively. **Row 1, 2, 3**: Traffic. **Row 4, 5**: Electricity. **Row 6, 7**: Exchange rate. The red background denotes the position of the location of the perturbation. The blue background denotes the output series.

Table 10: MLP structure

Input dim	Output dim	Activation
Length of sequence	96	LeakyReLU($\alpha = 0.2$)
96	96	LeakyReLU($\alpha = 0.2$)
96	96	LeakyReLU($\alpha = 0.2$)
96	96	LeakyReLU($\alpha = 0.2$)
96	Length of sequence	LeakyReLU($\alpha = 0.2$)

Table 11: LSTM/GRU structure

Number of layers	Hidden dim
4	32

Table 12: The structure of MLP-Mixer Block, and we stack 4 MLP-Mixer blocks to construct MLP-Mixer for forecasting and imputation.

Type	Input dim	Output dim	Activation
LayerNorm	96	96	/
Linear	128	128	GELU Hendrycks & Gimpel (2016)
Linear	128	128	GELU
LayerNorm	96	96	/
Linear	Length of sequence	Length of sequence	GELU
Linear	Length of sequence	Length of sequence	GELU

Table 13: The structure of Fully Convolutional Network (FCN) for TSC.

Layer	Input channel	Output channel	Kernel size
Conv1d	1	96	3
BatchNorm1d	96	96	N/A
ReLU	96	96	N/A
Conv1d	96	96	3
BatchNorm1d	96	96	N/A
ReLU	96	96	N/A
Conv1d	96	96	3
BatchNorm1d	96	96	N/A
ReLU	96	96	N/A
Conv1d	96	96	3
BatchNorm1d	96	96	N/A
ReLU	96	96	N/A
GlobalPooling	96	96	N/A
Linear	96	6	N/A

D Introduction to Pretrained Models

Model architecture. We use the classical forecasting and classification models, MLP, MLP-Mixer (Tolstikhin et al., 2021), GRU (Cho et al., 2014), LSTM (Hochreiter & Schmidhuber, 1997), FCN (Ismail Fawaz et al., 2019b) and ResNet-18 (He et al., 2016) as the pretrained models. We show the architecture of these models in Table 10, 11, 12, 13.

Training. we uniformly adapt Adam optimizer (Kingma & Ba, 2014) with $lr = 0.0001, \beta = (0.9, 0.999), \epsilon = 10^{-8}, \text{weight\_decay} = 0, \text{epochs} = 20$ for all the pretrained models.

E More Experimental Results

Comparison to peer methods on Mean Absolute Error (MAE). Table 15 compares MAE and FR of three defenses on Traffic. Analogous to the comparison (Table 2 in main paper) on MSE, MIA achieves both the lowest MAE and highest FR on $L_{\text{adv}} = 1\%, 2\%, 3\%$. DS outperforms MIA at $L_{\text{adv}} = 4\%, \ldots, 10\%$ for the great sacrifice on its FR.

Table 14: Comparison of imputation quality (MSE between the imputed series and the original series) of different imputation models on imputing the masked series of different mask length $L_{\text{mask}} = 5\%, 10\%, 15\%, 20\%$. Fixing L_{mask}, we first construct $t_0 - L_{\text{mask}} + 1$ masked series of L_{mask} and compute the average imputation MSE over imputing these $t_0 - L_{\text{mask}} + 1$ masked series. Bold indicates the best among four generators.

Generator	Traffic				Electricity				Exchange			
	5%	10%	15%	20%	5%	10%	15%	20%	5%	10%	15%	20%
MLP-Mixer	**0.0007**	**0.0082**	**0.0170**	**0.0240**	**0.0033**	**0.0320**	**0.0458**	**0.0631**	**0.0002**	**0.0028**	**0.0104**	**0.0212**
SAITS	0.0652	0.1110	0.1786	0.2476	0.0878	0.1654	0.2687	0.3586	0.0191	0.0410	0.0631	0.0824
Transformer	0.0642	0.1183	0.1854	0.2629	0.0821	0.1836	0.2404	0.3271	0.0210	0.0389	0.0595	0.0787
BRITS	0.0159	0.0419	0.0656	0.0927	0.0410	0.1192	0.1613	0.2109	0.0099	0.0252	0.0516	0.0705

Table 15: (Exchange) Comparison among three certified defenses on TSF dataset.

Metric	Defense	1 %	2 %	3 %	4 %	5 %	6 %	7 %	8 %	9 %	10 %
FR (%)	MIA ($L_{\text{mask}} = 10\%$)	**82.2**	**82.2**	**83.2**	**82.2**	**82.2**	**81.2**	**81.2**	**81.2**	**80.2**	**79.2**
	DS ($\eta = 10\%$)	24.8	24.8	24.8	24.8	24.8	24.8	24.8	24.8	24.8	24.8
	RA ($\eta = 10\%$)	16.8	16.8	16.8	16.8	16.8	16.8	16.8	16.8	16.8	16.8
	MIA ($L_{\text{mask}} = 15\%$)	**64.4**	**71.3**	**69.3**	**69.3**	**71.3**	**68.3**	**69.3**	**71.3**	**62.4**	**65.3**
	DS ($\eta = 15\%$)	20.8	20.8	20.8	14.9	14.9	11.9	11.9	11.9	11.9	10.9
	RA ($\eta = 15\%$)	23.8	23.8	23.8	23.8	23.8	23.8	23.8	23.8	23.8	23.8
MAE	MIA ($L_{\text{mask}} = 10\%$)	**0.332**	**0.330**	**0.334**	**0.330**	**0.330**	**0.327**	**0.326**	**0.326**	**0.323**	**0.320**
	DS ($\eta = 10\%$)	0.408	0.408	0.408	0.408	0.408	0.408	0.408	0.408	0.408	0.408
	RA ($\eta = 10\%$)	0.413	0.413	0.413	0.413	0.413	0.413	0.413	0.413	0.413	0.413
	MIA ($L_{\text{mask}} = 15\%$)	**0.307**	**0.320**	**0.313**	0.316	0.322	0.317	0.311	0.314	0.301	0.306
	DS ($\eta = 15\%$)	0.320	0.320	0.320	**0.215**	**0.215**	**0.222**	**0.222**	**0.222**	**0.222**	**0.204**
	RA ($\eta = 15\%$)	0.446	0.446	0.446	0.446	0.446	0.446	0.446	0.446	0.446	0.446

Table 16: (Traffic) The performance of MIA on different pretrained models. (c_1 $c_2\%$) reports (MAE, FR%) of MIA. **Baseline** is MAE of the pretrained model without MIA. The lowest MAE and the highest FR for each pretrained model is shown in bold-face.

Model	Baseline	L_{mask}	$\Delta = 1.0$			$\Delta = 1.2$			$\Delta = 1.5$		
			2%	5%	10%	2%	5%	10%	2%	5%	10%
MLP-Mixer	0.265	2%	**0.227** 72.3%			**0.213** 77.2%			0.340 89.1%		
		5%	0.231 75.2%	0.233 73.3%		0.225 **80.2%**	**0.218** 78.2%		**0.336** 90.1%	0.340 89.1%	
		10%	0.233 **77.2%**	**0.233** **76.2%**	**0.227** **69.3%**	0.225 **80.2%**	0.225 **80.2%**	**0.216** **76.2%**	0.338 **91.1%**	**0.336** **90.1%**	**0.333** **88.1%**
GRU	0.283	2%	**0.234** 66.3%			**0.210** 73.3%			**0.339** 89.1%		
		5%	0.242 72.3%	0.239 68.3%		0.219 76.2%	**0.214** 74.3%		0.340 **91.1%**	**0.337** 88.1%	
		10%	0.237 **74.3%**	**0.239** **72.3%**	**0.236** **63.4%**	0.217 **77.2%**	0.217 **77.2%**	**0.203** **70.3%**	0.340 **91.1%**	0.338 **90.1%**	**0.329** **86.1%**
LSTM	0.274	2%	**0.235** **66.3%**			**0.212** 76.2%			0.350 **91.1%**		
		5%	0.237 **66.3%**	**0.237** 65.3%		0.215 **77.2%**	**0.213** 76.2%		**0.345** 89.1%	**0.343** 88.1%	
		10%	0.237 65.3%	0.239 **66.3%**	**0.231** **61.4%**	0.215 **77.2%**	0.215 **77.2%**	**0.201** **72.3%**	0.347 89.1%	0.349 **90.1%**	**0.344** **87.1%**
MLP	0.268	2%	**0.226** 67.3%			**0.201** **72.3%**			0.344 90.1%		
		5%	0.231 **71.3%**	**0.226** 68.3%		**0.201** **72.3%**	**0.201** **72.3%**		0.343 **92.1%**	0.344 90.1%	
		10%	0.230 70.3%	0.230 **70.3%**	**0.225** **66.3%**	**0.201** **72.3%**	**0.201** **72.3%**	**0.199** **70.3%**	**0.341** 91.1%	**0.341** **91.1%**	**0.338** **89.1%**
ResNet18	0.290	2%	**0.244** 64.4%			0.238 75.2%			**0.343** 88.1%		
		5%	0.249 **68.3%**	**0.249** 65.3%		0.239 **79.2%**	0.241 **76.2%**		0.345 **89.1%**	**0.340** **87.1%**	
		10%	0.249 67.3%	0.251 **67.3%**	**0.246** **60.4%**	**0.235** 76.2%	**0.235** **76.2%**	**0.231** **73.3%**	0.345 88.1%	0.343 86.1%	**0.337** **83.2%**

Table 17: (Electricity) (c_1 $c_2\%$) report (MAE FR%) of MIA on different pretrained models.

Model	Baseline	L_{mask}	$\Delta = 1.0$			$\Delta = 1.2$			$\Delta = 1.5$		
			2%	5%	10%	2%	5%	10%	2%	5%	10%
MLP-Mixer	0.430	2%	**0.260** 66.3%			0.262 64.4%			0.312 77.2%		
		5%	0.264 **69.3%**	**0.262** **68.3%**		0.266 **67.3%**	0.263 **66.3%**		0.308 **78.2%**	0.308 **78.2%**	
		10%	0.264 67.3%	0.264 67.3%	**0.257** **55.4%**	**0.259** 64.4%	**0.259** 64.4%	**0.255** **59.4%**	**0.308** 77.2%	**0.308** 77.2%	**0.287** **66.3%**
GRU	0.441	2%	**0.269** 62.4%			**0.247** 60.4%			**0.312** 68.3%		
		5%	0.273 64.4%	0.274 **63.4%**		0.250 **62.4%**	**0.250** **62.4%**		0.317 **69.3%**	**0.317** **69.3%**	
		10%	0.275 **65.3%**	**0.270** 62.4%	**0.282** **49.5%**	0.247 61.4%	0.251 61.4%	**0.250** **53.5%**	0.317 **69.3%**	**0.317** **69.3%**	**0.295** **64.4%**
LSTM	0.447	2%	**0.273** 64.4%			**0.243** 52.5%			0.319 70.3%		
		5%	0.273 **66.3%**	0.275 **65.3%**		0.257 55.4%	**0.257** **55.4%**		**0.316** **71.3%**	**0.319** **70.3%**	
		10%	0.273 **66.3%**	**0.272** 64.4%	**0.298** **51.5%**	0.257 **56.4%**	**0.257** **55.4%**	**0.262** **48.5%**	**0.316** **71.3%**	0.320 **70.3%**	**0.294** **59.4%**
MLP	0.421	2%	0.283 73.3%			**0.242** 61.4%			0.313 74.3%		
		5%	0.287 **77.2%**	0.283 **75.2%**		0.249 **65.3%**	**0.245** **63.4%**		**0.304** **77.2%**	0.306 **76.2%**	
		10%	**0.283** 75.2%	**0.283** **75.2%**	**0.273** **60.4%**	0.250 61.4%	0.250 61.4%	**0.246** **55.4%**	**0.304** **77.2%**	**0.299** **76.2%**	**0.280** **66.3%**
ResNet18	0.569	2%	0.256 51.5%			0.243 59.4%			**0.318** 66.3%		
		5%	**0.248** 51.5%	**0.248** 50.5%		0.242 **60.4%**	**0.242** **60.4%**		0.324 **68.3%**	0.324 **68.3%**	
		10%	0.257 **52.5%**	0.256 **51.5%**	**0.255** **43.6%**	**0.240** 56.4%	0.244 58.4%	**0.237** **54.5%**	0.323 67.3%	**0.318** 66.3%	**0.302** **61.4%**

Evaluation of MAE on Traffic and Electricity. Table 16, Table 17 report MAE and FR of MIA on Traffic, Electricity and Exchange respectively, as a supplement to Table 4 and Table 5 in the main paper. We observe that MIA consistently reduces MAE of the pretrained models, similar to

Table 18: (Exchange) c_1 $c_2\%$ report MSE FR% of MIA at different L_{atk} and L_{def}.

Model	Baseline	L_{mask}	$\Delta = 1.0$			$\Delta = 1.2$			$\Delta = 1.5$		
			2%	5%	10%	2%	5%	10%	2%	5%	10%
MLP-Mixer	0.030	2%	0.060 **88.1%**			0.100 **87.1%**			0.158 **87.1%**		
		5%	**0.055** 83.2%	**0.053** 80.2%		0.096 84.2%	0.096 **84.2%**		0.144 83.2%	**0.138** 81.2%	
		10%	0.056 83.2%	0.053 **81.2%**	**0.051** **78.2%**	**0.095** 84.2%	**0.095** **84.2%**	**0.088** **80.2%**	**0.141** 82.2%	0.141 **82.2%**	**0.134** **79.2%**
GRU	0.040	2%	0.062 **83.2%**			0.104 83.2%			0.152 **84.2%**		
		5%	**0.060** 79.2%	**0.058** 75.2%		0.105 85.1%	**0.099** 80.2%		**0.150** 83.2%	**0.140** 77.2%	
		10%	0.061 82.2%	0.060 **80.2%**	**0.058** **68.3%**	**0.103** **86.1%**	0.100 **84.2%**	**0.098** **75.2%**	0.152 **84.2%**	0.152 **84.2%**	**0.142** **78.2%**
LSTM	0.042	2%	**0.061** **83.2%**			**0.098** **87.1%**			0.162 **85.1%**		
		5%	0.062 82.2%	**0.058** 78.2%		0.099 86.1%	**0.098** 83.2%		**0.159** 83.2%	**0.152** 79.2%	
		10%	0.063 82.2%	0.062 **80.2%**	**0.055** **75.2%**	0.099 86.1%	0.099 **85.1%**	**0.098** **82.2%**	0.160 84.2%	0.160 **84.2%**	**0.155** **82.2%**
MLP	0.658	2%	0.065 **27.7%**			0.110 41.6%			0.210 **56.4%**		
		5%	**0.057** 26.7%	0.072 19.8%		**0.105** **44.6%**	**0.094** 27.7%		**0.209** 53.5%	0.231 40.6%	
		10%	**0.057** 26.7%	**0.057** **26.7%**	**0.069** **18.8%**	0.107 **44.6%**	0.106 **43.6%**	**0.105** **35.6%**	0.213 51.5%	**0.216** **52.5%**	**0.240** **39.6%**
ResNet18	0.053	2%	0.060 78.2%			0.096 **83.2%**			0.163 **88.1%**		
		5%	**0.058** **79.2%**	**0.058** 77.2%		0.093 81.2%	0.093 **80.2%**		**0.163** 87.1%	**0.157** 85.1%	
		10%	0.058 78.2%	0.060 **78.2%**	**0.059** **72.3%**	**0.091** 78.2%	**0.092** 78.2%	**0.090** **76.2%**	**0.163** 87.1%	0.163 **87.1%**	**0.159** **85.1%**

Table 19: (Exchange) c_1 $c_2\%$ report MAE FR% of MIA at different L_{adv} and L_{mask}.

Model	Baseline	L_{mask}	$\Delta = 1.0$			$\Delta = 1.2$			$\Delta = 1.5$		
			2%	5%	10%	2%	5%	10%	2%	5%	10%
MLP-Mixer	0.133	2%	0.209 **88.1%**			0.270 **87.1%**			0.349 **87.1%**		
		5%	**0.199** 83.2%	**0.194** 80.2%		0.264 84.2%	0.264 **84.2%**		0.333 83.2%	**0.326** 81.2%	
		10%	0.200 83.2%	0.195 **81.2%**	**0.190** **78.2%**	**0.263** 84.2%	**0.263** **84.2%**	**0.252** **80.2%**	**0.330** 82.2%	0.330 **82.2%**	**0.320** **79.2%**
GRU	0.152	2%	0.211 **83.2%**			**0.274** 83.2%			0.342 **84.2%**		
		5%	**0.206** 79.2%	**0.203** 75.2%		0.276 85.1%	**0.267** 80.2%		**0.339** 83.2%	**0.325** 77.2%	
		10%	0.210 82.2%	0.209 **80.2%**	**0.203** **68.3%**	0.274 **86.1%**	0.270 **84.2%**	**0.263** **75.2%**	0.342 **84.2%**	0.342 **84.2%**	**0.330** **78.2%**
LSTM	0.159	2%	**0.209** **83.2%**			**0.266** **87.1%**			0.352 **85.1%**		
		5%	0.210 82.2%	**0.203** 78.2%		0.266 86.1%	**0.264** 83.2%		**0.348** 83.2%	**0.340** 79.2%	
		10%	0.213 82.2%	0.211 **80.2%**	**0.199** **75.2%**	0.266 86.1%	0.266 **85.1%**	**0.263** **82.2%**	0.350 84.2%	0.350 **84.2%**	**0.344** **82.2%**
MLP	0.639	2%	0.213 **27.7%**			0.284 41.6%			0.409 **56.4%**		
		5%	**0.196** 26.7%	0.229 19.8%		**0.274** **44.6%**	**0.260** 27.7%		**0.405** 53.5%	0.447 40.6%	
		10%	**0.196** 26.7%	**0.196** **26.7%**	**0.227** **18.8%**	0.277 **44.6%**	0.274 **43.6%**	**0.275** **35.6%**	0.412 51.5%	**0.416** **52.5%**	**0.458** **39.6%**
ResNet18	0.181	2%	0.205 78.2%			0.263 **83.2%**			0.355 **88.1%**		
		5%	**0.201** **79.2%**	**0.201** 77.2%		0.257 81.2%	0.257 **80.2%**		**0.354** 87.1%	**0.347** 85.1%	
		10%	0.202 78.2%	0.205 **78.2%**	**0.201** **72.3%**	**0.254** 78.2%	**0.256** 78.2%	**0.253** **76.2%**	**0.354** 87.1%	0.354 **87.1%**	**0.349** **85.1%**

the results on MSE. Our comprehensive experiments suggest that MIA can effectively improve our forecasting quality in the way of filtering the unconfident forecasts.

Evaluation of MSE and MAE for MIA on Exchange. Table 18 and Table 19 evaluate MSE/MAE of MIA on exchange. We observe that, MIA moderately increase MSE/MAE of the pretrained models because of the information loss for the discretization technique. Specifically, we can see that MSE/MAE of the pretrained models are commonly much smaller than that of Traffic and Electricity because Exchange dataset is much simpler. The better forecasting performance implies that we might lose more information for the discretization technique. On Exchange, information loss plays a more conspicuous role than the filtering function of MIA, causing the increase of MSE/MAE. This suggests that discretization technique might lower the forecasting performance when the pretrained models are precise enough.

Analysis of training algorithm of imputation models. Table 20 reportS MSE and FR of masked training and random training on the TSF dataset Traffic. Similar to the comparison on TSC datasets (Table 6 in the main paper), our masked training consistently achieves lower MSE than random training on different imputation models.

Analysis of Different Pretrained Models on MIA. Table 21 reports the MAE of MIA with different pretrained models, as a supplement to Table 7 in the main paper. The results demonstrate that MLP-Mixer outperforms all the other defenses.

F MIA on Multivariate Time Series Forecasting (MTSF)

Apply MIA to Multivariate. Suppose the input series is a d_0-dimension t_0-length matrix $\mathcal{X} \in \mathbb{R}^{t_0 \times d_0}$. We can represent the multivariate series uniquely by d_0 univariate series $\mathbf{x}_{1:t_0}^{(d)}, d = 1, 2, \ldots, d_0$.

$$\mathcal{X} = [\mathbf{x}_{1:t_0}^{(1)},\ \mathbf{x}_{2:t_0}^{(2)},\ \ldots,\ \mathbf{x}_{1:t_0}^{(d_0)}]^T \tag{23}$$

Table 20: (Traffic) Comparison between mask methods. c_1 $c_2\%$ report MSE TPR% of MIA across $L_{\text{def}} = 2\%, 5\%, 10\%$, $L_{\text{atk}} = 2\%, 5\%, 10\%$, $\Delta = 1.0, 1.2, 1.5$. c_1. MSE(c_1) reports the forecasting performance.

Model	Mask Method	L_{mask}	$\Delta = 1.0$			$\Delta = 1.2$			$\Delta = 1.5$		
			2%	5%	10%	2%	5%	10%	2%	5%	10%
GRU	random	2%	**0.068** 53.5%			**0.071** 63.4%			**0.144** 76.2%		
		5%	**0.071** 42.6%	0.075 28.7%		**0.063** 50.5%	**0.057** 43.6%		**0.145** 73.3%	**0.135** 62.4%	
		10%	0.073 30.7%	**0.069** 26.7%	0.075 23.8%	**0.052** 49.5%	**0.048** 45.5%	**0.051** 40.6%	**0.140** 66.3%	**0.138** 64.4%	**0.132** 59.4%
	block	2%	0.074 **64.4%**			0.073 **66.3%**			0.148 **84.2%**		
		5%	0.073 **66.3%**	**0.075** **61.4%**		0.073 **66.3%**	0.073 **65.3%**		0.148 **83.2%**	0.145 **80.2%**	
		10%	**0.073** **64.4%**	0.074 **63.4%**	**0.070** **57.4%**	0.074 **65.3%**	0.074 **64.4%**	0.065 **59.4%**	0.148 **84.2%**	0.148 **84.2%**	0.145 **79.2%**
LSTM	random	2%	**0.064** 55.4%			0.073 62.4%			0.144 81.2%		
		5%	**0.063** 37.6%	**0.050** 25.7%		**0.051** 49.5%	**0.055** 38.6%		**0.129** 67.3%	**0.130** 58.4%	
		10%	**0.065** 37.6%	**0.053** 27.7%	**0.049** 14.9%	**0.050** 48.5%	**0.053** 45.5%	**0.046** 30.7%	**0.134** 68.3%	**0.128** 64.4%	**0.120** 53.5%
	block	2%	0.071 **61.4%**			**0.069** **68.3%**			**0.144** **85.1%**		
		5%	0.067 **59.4%**	0.067 **56.4%**		0.069 **68.3%**	0.068 **66.3%**		0.144 **85.1%**	0.141 **82.2%**	
		10%	0.068 **60.4%**	0.067 **58.4%**	0.067 **56.4%**	0.069 **67.3%**	0.069 **66.3%**	0.067 **65.3%**	0.144 **85.1%**	0.144 **85.1%**	0.142 **83.2%**
MLP-Mixer	random	2%	**0.073** 54.5%			0.085 66.3%			**0.147** 75.2%		
		5%	**0.074** 44.6%	**0.067** 27.7%		**0.072** 59.4%	**0.061** 47.5%		**0.137** 74.3%	**0.142** 63.4%	
		10%	**0.072** 42.6%	**0.073** 40.6%	**0.059** 26.7%	**0.065** 57.4%	**0.067** 53.5%	**0.061** 43.6%	**0.134** 74.3%	**0.130** 70.3%	**0.130** 61.4%
	block	2%	0.079 **67.3%**			**0.085** **74.3%**			0.151 **86.1%**		
		5%	0.076 **67.3%**	0.078 **61.4%**		0.083 **76.2%**	0.079 **72.3%**		0.151 **86.1%**	0.149 **83.2%**	
		10%	0.079 **63.4%**	0.077 **61.4%**	0.076 **55.4%**	0.081 **72.3%**	0.077 **71.3%**	0.078 **69.3%**	0.151 **86.1%**	0.150 **85.1%**	0.145 **82.2%**
MLP	random	2%	**0.069** 53.5%			0.074 61.4%			**0.145** 75.2%		
		5%	0.072 44.6%	0.071 37.6%		**0.059** 58.4%	**0.044** 47.5%		**0.138** 78.2%	**0.138** 67.3%	
		10%	**0.072** 42.6%	0.073 40.6%	0.077 34.7%	**0.061** 53.5%	**0.062** 52.5%	**0.055** 48.5%	**0.140** 78.2%	**0.140** 75.2%	**0.133** 67.3%
	block	2%	0.072 **60.4%**			**0.068** **68.3%**			0.146 **84.2%**		
		5%	**0.071** **61.4%**	**0.071** **58.4%**		0.070 **66.3%**	0.070 **66.3%**		0.145 **86.1%**	0.147 **85.1%**	
		10%	0.073 **58.4%**	**0.072** **59.4%**	**0.069** **52.5%**	0.065 **66.3%**	0.065 **66.3%**	0.065 **62.4%**	0.146 **84.2%**	0.147 **85.1%**	0.144 **82.2%**
ResNet18	random	2%	**0.071** 57.4%			**0.083** 66.3%			**0.143** 82.2%		
		5%	**0.073** 33.7%	**0.072** 29.7%		**0.063** 54.5%	**0.057** 46.5%		**0.136** 62.4%	**0.139** 55.4%	
		10%	**0.067** 32.7%	**0.070** 27.7%	0.076 17.8%	**0.059** 49.5%	**0.061** 49.5%	**0.047** 37.6%	**0.143** 61.4%	**0.130** 53.5%	**0.117** 45.5%
	block	2%	0.073 **63.4%**			0.089 **71.3%**			0.146 **86.1%**		
		5%	0.074 **62.4%**	0.074 **62.4%**		0.085 **68.3%**	0.084 **67.3%**		0.147 **87.1%**	0.146 **86.1%**	
		10%	0.075 **60.4%**	0.072 **59.4%**	**0.070** **57.4%**	0.087 **68.3%**	0.084 **69.3%**	0.076 **62.4%**	0.143 **84.2%**	0.143 **84.2%**	0.140 **82.2%**

Table 21: Comparison of four imputation models. The best results are shown in bold-face.

Generator	Metric	L_{mask}	Electricity			Exchange			Traffic		
			2%	5%	10%	2%	5%	10%	2%	5%	10%
MLP-Mixer	MAE	2%	0.312 **77.2%**			0.349 **87.1%**			0.340 **89.1%**		
		5%	0.308 **78.2%**	0.308 **78.2%**		0.333 **83.2%**	0.326 **81.2%**		0.336 **90.1%**	0.340 **89.1%**	
		10%	0.308 **77.2%**	0.308 **77.2%**	0.287 **66.3%**	0.330 **82.2%**	0.330 **82.2%**	0.320 **79.2%**	0.338 **91.1%**	0.336 **90.1%**	0.333 **88.1%**
BRITS	MAE	2%	0.290 65.3%			0.299 40.6%			0.338 87.1%		
		5%	0.283 71.3%	0.264 59.4%		0.288 49.5%	0.246 15.8%		0.327 84.2%	0.320 75.2%	
		10%	0.271 61.4%	0.272 60.4%	0.265 45.5%	0.381 10.9%	0.526 1.0%	Inf 0.0%	0.315 79.2%	0.319 77.2%	0.312 73.3%
SAITS	MAE	2%	0.269 58.4%			**0.258** 25.7%			**0.307** 67.3%		
		5%	**0.261** 53.5%	**0.256** 52.5%		0.317 43.6%	0.264 27.7%		0.321 73.3%	**0.308** 68.3%	
		10%	0.274 56.4%	0.278 54.5%	**0.263** 44.6%	0.179 7.9%	**0.123** 6.9%	**0.035** 4.0%	0.316 67.3%	0.325 69.3%	0.315 59.4%
Transformer	MAE	2%	**0.253** 52.5%			0.329 23.8%			0.322 68.3%		
		5%	0.288 52.5%	0.291 42.6%		**0.164** 6.9%	**0.030** 2.0%		**0.318** 74.3%	0.312 65.3%	
		10%	**0.266** 60.4%	**0.263** 58.4%	0.274 34.7%	**0.112** 8.9%	0.135 7.9%	0.037 5.0%	**0.313** 75.2%	**0.317** 74.3%	**0.312** 61.4%

1. We generate the masks in the same way as **Masking (Step 1)**. The main difference is the way we mask the multivariate series with the univariate mask. Masking multivariate series $\mathcal{X}$ with the mask $\mathrm{M}_{[u:v]}$ is computed as follow:

$$\mathcal{X} \odot \mathrm{M}_{[u:v]} = \left[\mathbf{x}_{1:t_0}^{(1)} \odot \mathrm{M}_{[u:v]},\ \mathbf{x}_{2:t_0}^{(2)} \odot \mathrm{M}_{[u:v]},\ \ldots, \mathbf{x}_{1:t_0}^{(d_0)} \odot \mathrm{M}_{[u:v]}\right]^T \tag{24}$$

2. With the imputation model $G(\cdot)$, **Imputing (Step 2)** for multivariate series $\mathcal{X}$ is computed as follow:

$$G(\mathcal{X} \odot \mathrm{M}_{[u:v]}) = \left[G\left(\mathbf{x}_{1:t_0}^{(1)} \odot \mathrm{M}_{[u:v]}\right),\ G\left(\mathbf{x}_{2:t_0}^{(2)} \odot \mathrm{M}_{[u:v]}\right),\ \ldots,\ G\left(\mathbf{x}_{1:t_0}^{(d_0)} \odot \mathrm{M}_{[u:v]}\right)\right]^T \tag{25}$$

3. We aggregate all the predictions of the imputed multivariate series in the same way as **Aggregation (Step 3)** for univariate series.

Evaluation of MIA on multivariate tasks. In terms of the multivariate time series forecasting (MTSF) task, we follow the work (Wu et al., 2021) and evaluate our MIA framework on four datasets (ETTh2 (Zhou et al., 2021), ETTm2 (Zhou et al., 2021), weather [8] and illness [9]. Corresponding results are presented in Table 22 to 29. Extensive experiments demonstrate that MIA behaves similarly to that of univariate forecasting tasks.

[8] https://www.bgc-jena.mpg.de/wetter/

[9] https://gis.cdc.gov/grasp/fluview/fluportaldashboard.html

Table 22: (ETTh2) Evaluate MAE of MIA with pretrained models on multi-variate time series forecasting (MTSF).

Model	Baseline	L_{mask}	$\Delta = 1.0$			$\Delta = 1.2$			$\Delta = 1.5$		
			2 %	5 %	10 %	2 %	5 %	10 %	2 %	5 %	10 %
MLP-Mixer	0.712	2 %	0.363 74.9%			0.434 82.4%			0.550 90.3%		
		5 %	0.363 **75.8%**	0.360 73.8%		0.435 **83.6%**	0.432 81.8%		0.552 **90.8%**	0.547 89.8%	
		10 %	**0.360** 75.0%	**0.356 74.2%**	**0.346 70.1%**	**0.431** 82.6%	**0.427 82.2%**	**0.415 77.5%**	**0.548** 90.5%	**0.542 90.1%**	**0.528 86.9%**
MLP	0.815	2 %	**0.368** 68.4%			**0.436** 76.5%			**0.542** 85.5%		
		5 %	0.371 **69.0%**	0.365 **66.7%**		0.438 **76.6%**	**0.434** 75.5%		0.547 **86.6%**	**0.541** 85.1%	
		10 %	0.368 67.0%	**0.365** 66.5%	**0.356 64.4%**	0.438 76.1%	0.435 **75.9%**	**0.424 73.3%**	0.545 86.3%	0.541 **85.8%**	**0.527 83.5%**
LSTM	0.802	2 %	0.374 **69.1%**			**0.444** 76.6%			**0.556** 85.7%		
		5 %	0.375 68.7%	**0.372** 67.9%		0.447 **77.1%**	0.443 **76.0%**		0.558 **85.9%**	0.552 84.7%	
		10 %	**0.373** 68.4%	0.373 **68.0%**	**0.370 66.7%**	0.445 76.7%	**0.443 76.0%**	**0.436 74.0%**	0.556 **85.9%**	**0.551 85.2%**	**0.542 83.6%**
GRU	0.782	2 %	0.373 71.6%			0.441 78.1%			0.563 87.1%		
		5 %	0.374 **72.4%**	**0.371** 70.0%		0.442 **78.3%**	0.440 77.2%		0.565 **87.6%**	0.560 85.9%	
		10 %	**0.372** 72.0%	0.372 **71.6%**	**0.369 68.1%**	**0.440** 78.0%	**0.439 77.6%**	**0.435 75.4%**	**0.562** 87.3%	**0.556 86.9%**	**0.545 84.2%**
RNN	0.809	2 %	0.384 69.9%			0.454 79.0%			0.560 **87.6%**		
		5 %	0.383 **70.2%**	0.382 **68.8%**		0.454 **79.2%**	0.453 **78.4%**		0.560 **87.6%**	0.559 **87.0%**	
		10 %	**0.381** 69.3%	**0.380** 68.4%	**0.378 67.1%**	**0.452** 78.7%	**0.451** 78.3%	**0.448 76.9%**	**0.559** 87.5%	**0.556 87.0%**	**0.551 86.1%**
TransformerNormal	0.852	2 %	0.405 **67.0%**			0.481 **75.2%**			0.593 **83.8%**		
		5 %	0.404 66.6%	0.403 **66.1%**		0.480 75.1%	0.480 **74.8%**		0.592 83.4%	0.591 **83.3%**	
		10 %	**0.400** 65.1%	**0.397** 64.6%	**0.393 63.1%**	**0.478** 74.5%	**0.477** 74.3%	**0.473 73.4%**	**0.589** 83.1%	**0.587** 82.4%	**0.583 81.9%**
TransformerPadding	0.981	2 %	0.346 **57.9%**			0.427 65.3%			0.553 **76.7%**		
		5 %	0.346 57.8%	0.346 **57.8%**		0.426 65.3%	0.426 65.3%		0.552 76.5%	0.552 **76.5%**	
		10 %	**0.344** 57.8%	**0.344 57.8%**	**0.344 57.8%**	**0.425 65.4%**	**0.425 65.4%**	**0.424 65.3%**	**0.550** 76.5%	**0.550 76.5%**	**0.550 76.5%**
TransformerConv	0.934	2 %	0.353 **61.1%**			0.427 70.2%			0.538 **79.4%**		
		5 %	0.352 61.0%	0.351 **60.6%**		0.426 **70.3%**	0.424 **69.7%**		0.537 **79.4%**	0.536 **79.4%**	
		10 %	**0.350** 60.2%	**0.349** 60.1%	**0.348 59.7%**	**0.423** 69.7%	**0.423** 69.6%	**0.419 68.7%**	**0.535** 79.3%	**0.534** 79.3%	**0.531 79.1%**

Table 23: (ETTh2) Evaluate MSE of MIA with different pretrained models on multi-variate time series forecasting (MTSF).

Model	Baseline	L_{mask}	$\Delta = 1.0$			$\Delta = 1.2$			$\Delta = 1.5$		
			2 %	5 %	10 %	2 %	5 %	10 %	2 %	5 %	10 %
MLP-Mixer	0.930	2 %	0.159 74.9%			0.230 82.4%			0.367 90.3%		
		5 %	0.159 **75.8%**	0.157 73.8%		0.231 **83.6%**	0.228 81.8%		0.370 **90.8%**	0.365 89.8%	
		10 %	**0.157** 75.0%	**0.155 74.2%**	**0.149 70.1%**	**0.228** 82.6%	**0.225 82.2%**	**0.215 77.5%**	**0.366** 90.5%	**0.360 90.1%**	**0.347 86.9%**
MLP	1.143	2 %	0.162 68.4%			**0.230** 76.5%			**0.357** 85.5%		
		5 %	0.163 **69.0%**	0.160 **66.7%**		0.231 **76.6%**	**0.228** 75.5%		0.362 **86.6%**	**0.356** 85.1%	
		10 %	**0.162** 67.0%	**0.159** 66.5%	**0.153 64.4%**	0.230 76.1%	0.228 **75.9%**	**0.219 73.3%**	0.360 86.3%	0.357 **85.8%**	**0.342 83.5%**
LSTM	1.072	2 %	0.165 **69.1%**			**0.235** 76.6%			0.370 85.7%		
		5 %	0.165 68.7%	**0.164** 67.9%		0.237 **77.1%**	0.234 **76.0%**		0.371 **85.9%**	0.366 84.7%	
		10 %	**0.164** 68.4%	0.164 **68.0%**	**0.162 66.7%**	0.236 76.7%	**0.233 76.0%**	**0.228 74.0%**	**0.369 85.9%**	**0.365 85.2%**	**0.357 83.6%**
GRU	1.042	2 %	0.166 71.6%			0.236 78.1%			0.378 87.1%		
		5 %	0.167 **72.4%**	**0.165** 70.0%		0.237 **78.3%**	0.235 77.2%		0.380 **87.6%**	0.376 85.9%	
		10 %	**0.166** 72.0%	0.165 **71.6%**	**0.161 68.1%**	**0.235** 78.0%	**0.233 77.6%**	**0.229 75.4%**	**0.377** 87.3%	**0.373 86.9%**	**0.364 84.2%**
RNN	1.074	2 %	0.171 69.9%			0.244 79.0%			0.375 **87.6%**		
		5 %	0.171 **70.2%**	0.170 **68.8%**		0.243 **79.2%**	0.243 **78.4%**		0.375 **87.6%**	0.373 **87.0%**	
		10 %	**0.170** 69.3%	**0.169** 68.4%	**0.166 67.1%**	**0.242** 78.7%	**0.241** 78.3%	**0.238 76.9%**	**0.373** 87.5%	**0.370 87.0%**	**0.366 86.1%**
TransformerNormal	1.241	2 %	0.186 **67.0%**			0.264 **75.2%**			0.406 **83.8%**		
		5 %	0.185 66.6%	0.184 **66.1%**		0.263 75.1%	0.262 **74.8%**		0.404 83.4%	0.403 **83.3%**	
		10 %	**0.182** 65.1%	**0.180** 64.6%	**0.177 63.1%**	**0.261** 74.5%	**0.259** 74.3%	**0.256 73.4%**	**0.401** 83.1%	**0.398** 82.4%	**0.394 81.9%**
TransformerPadding	1.576	2 %	0.149 **57.9%**			0.222 65.3%			0.362 **76.7%**		
		5 %	0.149 57.8%	0.149 **57.8%**		0.222 65.3%	0.222 65.3%		0.361 76.5%	0.361 **76.5%**	
		10 %	**0.148** 57.8%	**0.148 57.8%**	**0.148 57.8%**	**0.221 65.4%**	**0.221 65.4%**	**0.221 65.3%**	**0.359** 76.5%	**0.359 76.5%**	**0.359 76.5%**
TransformerConv	1.424	2 %	0.154 **61.1%**			0.224 70.2%			0.353 **79.4%**		
		5 %	0.154 61.0%	0.153 **60.6%**		0.224 **70.3%**	0.222 **69.7%**		0.352 **79.4%**	0.351 **79.4%**	
		10 %	**0.153** 60.2%	**0.152** 60.1%	**0.151 59.7%**	**0.222** 69.7%	**0.221** 69.6%	**0.219 68.7%**	**0.350** 79.3%	**0.349** 79.3%	**0.347 79.1%**

G Imputation Models.

For the imputation model architectures, we take SAITS, Transformer and BRITS and MLP-Mixer. Specifically, for SAITS, we use the code from [10]. For SAITS (Du et al., 2022), we set $d_{\text{model}} = 32, n_{\text{layers}} = 2, d_{\text{inner}} = 16, n_{\text{head}} = 4, d_{\text{k}} = 8, d_{\text{v}} = 8$. For Transformer (Vaswani et al., 2017), we set $d_{\text{model}} = 32, n_{\text{layers}} = 2, d_{\text{inner}} = 16, n_{\text{head}} = 4, d_{\text{k}} = 8, d_{\text{v}} = 8$. For BRITS (Cao et al., 2018), we set $h_{\text{hidden}} = 32$. For MLP-Mixer (Tolstikhin et al., 2021), we use the same structure as Table 12. In terms of training, we use optimizer Adam with $lr = 0.0001, \beta = (0.9, 0.999), \epsilon = 10^{-8}$, weight_decay $= 0$ and train the model for 30 epochs.

G.1 Choice of Imputation Model Architecture.

Table 14 compares the imputation quality of different imputation models on Traffic. The imputation quality is quantified by the mean square error (MSE) between the imputed series and the original series. We observe that MLP-Mixer consistently outperforms other three models across different datasets and L_{adv}, indicating the superior imputation ability of MLP-Mixer architecture.

[10] https://github.com/WenjieDu/PyPOTS

Table 24: (ETTm2) Evaluate MAE of MIA with different pretrained models on multi-variate time series forecasting (MTSF).

Model	Baseline	L_{mask}	$\Delta = 1.0$			$\Delta = 1.2$			$\Delta = 1.5$		
			2 %	5 %	10 %	2 %	5 %	10 %	2 %	5 %	10 %
MLP-Mixer	0.858	2 %	**0.329** 67.6%			**0.404** 75.5%			**0.526** 83.7%		
		5 %	0.340 **68.2%**	**0.312** 62.3%		0.421 **76.1%**	**0.385** 70.7%		0.548 **84.3%**	**0.504** 80.1%	
		10 %	0.337 67.2%	0.336 **66.7%**	**0.299 56.4%**	0.414 75.3%	0.411 **75.0%**	**0.361 65.0%**	0.538 82.9%	0.533 **82.8%**	**0.467 75.6%**
MLP	0.755	2 %	**0.350** 74.2%			**0.427** 82.0%			**0.546** 86.5%		
		5 %	0.366 **76.3%**	**0.325** 70.2%		0.453 **85.1%**	**0.408** 80.7%		0.577 **87.4%**	**0.527** 86.0%	
		10 %	0.357 74.6%	0.351 **72.0%**	**0.324 61.9%**	0.445 83.8%	0.440 **82.4%**	**0.411 72.5%**	0.569 86.8%	0.567 **87.0%**	**0.529 80.8%**
LSTM	1.034	2 %	0.364 **64.6%**			0.462 **72.9%**			0.594 **82.4%**		
		5 %	0.363 64.2%	0.357 **63.9%**		0.460 72.1%	0.454 **71.3%**		0.594 81.9%	**0.589** 81.6%	
		10 %	**0.359** 63.8%	**0.355** 63.2%	**0.347 62.1%**	**0.456** 71.3%	**0.452** 70.6%	**0.444 69.2%**	**0.591** 81.7%	0.589 **81.8%**	**0.583 81.4%**
GRU	1.065	2 %	0.388 **62.4%**			0.479 **69.9%**			0.619 **78.9%**		
		5 %	0.388 61.8%	**0.371 60.2%**		0.479 69.6%	**0.463 67.6%**		0.620 78.3%	**0.604** 76.8%	
		10 %	**0.382** 59.9%	0.375 59.0%	**0.353 54.7%**	**0.476** 67.5%	0.468 66.5%	**0.445 62.3%**	**0.616** 77.2%	0.610 **77.1%**	**0.589 74.2%**
RNN	1.024	2 %	**0.299** 61.7%			**0.363** 70.1%			**0.462** 77.4%		
		5 %	0.310 64.2%	**0.273** 56.9%		0.375 **71.6%**	**0.338** 65.6%		0.481 **78.2%**	**0.448** 73.3%	
		10 %	0.308 **64.6%**	0.299 **60.5%**	**0.260 49.7%**	0.372 **71.6%**	0.358 **68.0%**	**0.310 59.9%**	0.478 77.6%	0.465 **75.2%**	**0.410 69.5%**
TransformerNormal	0.989	2 %	0.322 **57.7%**			0.382 **67.5%**			0.468 **77.6%**		
		5 %	0.318 56.5%	0.309 51.2%		0.382 66.8%	0.369 61.8%		0.473 76.4%	**0.455** 73.8%	
		10 %	**0.311** 53.4%	**0.305 51.4%**	**0.283 41.0%**	**0.377** 64.5%	**0.369 62.4%**	**0.353 54.6%**	**0.466** 75.7%	0.457 **74.1%**	**0.435 68.7%**
TransformerPadding	1.096	2 %	0.376 **51.8%**			**0.445 60.7%**			0.559 **73.3%**		
		5 %	0.392 48.5%	0.393 **44.0%**		0.459 59.5%	0.459 **54.0%**		**0.552** 71.4%	**0.551 68.3%**	
		10 %	**0.374** 38.2%	**0.377** 34.8%	**0.373 27.0%**	0.447 48.5%	**0.445** 46.1%	**0.434 37.3%**	0.556 63.0%	0.553 61.6%	**0.543 54.6%**
TransformerConv	0.869	2 %	0.331 **67.5%**			0.401 72.3%			0.519 78.8%		
		5 %	0.314 66.7%	**0.294** 58.9%		0.390 **72.8%**	**0.362** 66.4%		0.511 **79.2%**	**0.478 75.3%**	
		10 %	**0.312** 61.7%	0.308 **60.0%**	**0.298 50.4%**	**0.384** 68.8%	0.375 **66.5%**	**0.362 58.7%**	**0.504** 77.5%	0.488 75.1%	**0.467 68.4%**

Table 25: (ETTm2) Evaluate MSE of MIA with different pretrained models on multi-variate time series forecasting (MTSF).

Model	Baseline	L_{mask}	$\Delta = 1.0$			$\Delta = 1.2$			$\Delta = 1.5$		
			2 %	5 %	10 %	2 %	5 %	10 %	2 %	5 %	10 %
MLP-Mixer	1.750	2 %	**0.139** 67.6%			**0.206** 75.5%			**0.339** 83.7%		
		5 %	0.145 **68.2%**	**0.128** 62.3%		0.219 **76.1%**	**0.192** 70.7%		0.362 **84.3%**	**0.319** 80.1%	
		10 %	0.143 67.2%	0.142 **66.7%**	**0.121 56.4%**	0.214 75.3%	0.212 **75.0%**	**0.176 65.0%**	0.352 82.9%	0.348 **82.8%**	**0.287 75.6%**
MLP	1.508	2 %	**0.149** 74.2%			**0.222** 82.0%			**0.358** 86.5%		
		5 %	0.161 **76.3%**	**0.134** 70.2%		0.243 **85.1%**	**0.208** 80.7%		0.385 **87.4%**	**0.337** 86.0%	
		10 %	0.156 74.6%	0.152 **72.0%**	**0.134 61.9%**	0.237 83.8%	0.233 **82.4%**	**0.211 72.5%**	0.377 86.8%	0.376 **87.0%**	**0.336 80.8%**
LSTM	2.858	2 %	0.158 **64.6%**			0.242 **72.9%**			0.391 **82.4%**		
		5 %	0.157 64.2%	0.154 **63.9%**		0.241 72.1%	0.236 **71.3%**		0.391 81.9%	0.386 81.6%	
		10 %	**0.155** 63.8%	**0.152** 63.2%	**0.149 62.1%**	**0.238** 71.3%	**0.235** 70.6%	**0.229 69.2%**	**0.387** 81.7%	**0.386 81.8%**	**0.381 81.4%**
GRU	2.685	2 %	0.174 **62.4%**			0.260 **69.9%**			0.426 **78.9%**		
		5 %	0.174 61.8%	**0.163 60.2%**		0.261 69.6%	**0.247 67.6%**		0.426 78.3%	**0.410** 76.8%	
		10 %	**0.171** 59.9%	0.168 59.0%	**0.154 54.7%**	**0.260** 67.5%	0.254 66.5%	**0.236 62.3%**	**0.422** 77.2%	0.417 **77.1%**	**0.395 74.2%**
RNN	2.598	2 %	**0.121** 61.7%			**0.177** 70.1%			**0.280** 77.4%		
		5 %	0.127 64.2%	**0.104** 56.9%		0.185 **71.6%**	**0.159** 65.6%		0.297 **78.2%**	**0.266** 73.3%	
		10 %	0.125 **64.6%**	0.120 **60.5%**	**0.096 49.7%**	0.183 **71.6%**	0.173 **68.0%**	**0.138 59.9%**	0.295 77.6%	0.285 **75.2%**	**0.233 69.5%**
TransformerNormal	2.150	2 %	0.131 **57.7%**			0.186 **67.5%**			0.286 **77.6%**		
		5 %	0.128 56.5%	0.121 51.2%		0.187 66.8%	0.174 61.8%		0.288 76.4%	0.269 73.8%	
		10 %	**0.124** 53.4%	**0.120 51.4%**	**0.108 41.0%**	**0.181** 64.5%	**0.173 62.4%**	**0.163 54.6%**	**0.279** 75.7%	**0.268 74.1%**	**0.249 68.7%**
TransformerPadding	2.828	2 %	0.168 **51.8%**			0.238 **60.7%**			0.375 **73.3%**		
		5 %	0.175 48.5%	0.174 **44.0%**		0.245 59.5%	0.243 **54.0%**		0.369 71.4%	0.367 **68.3%**	
		10 %	**0.166** 38.2%	**0.168** 34.8%	**0.164 27.0%**	**0.236** 48.5%	**0.235** 46.1%	**0.226 37.3%**	**0.367** 63.0%	**0.365** 61.6%	**0.353 54.6%**
TransformerConv	1.918	2 %	0.139 **67.5%**			0.203 72.3%			0.332 78.8%		
		5 %	0.129 66.7%	**0.118** 58.9%		0.195 **72.8%**	**0.175** 66.4%		0.323 **79.2%**	**0.291 75.3%**	
		10 %	**0.128** 61.7%	0.124 **60.0%**	**0.117 50.4%**	**0.192** 68.8%	0.184 **66.5%**	**0.174 58.7%**	**0.318** 77.5%	0.304 75.1%	**0.283 68.4%**

G.2 Impact of Gaussian Augmentation

Table 33, Table 34, Table 35, Table 36 and Table 37 report the impact of Gaussian augmentation at $\sigma = 0.01, 0.02, 0.03, 0.04, 0.05$ on time series classification dataset DistalPhalanxTW ($L_{mask} = 15\%$) respectively. We compare the MIA with Gaussian augmentation to MIA without Gaussian augmentation (baseline) on **Certified Accuracy** at $L_{atk} = 5\%, 10\%, 15\%$. The table reports the relative improvement (abs $\%$) on certified accuracy.

G.3 Visualize the imputation quality.

Fig. 4 intuitively shows the imputation performance of different imputation models on dataset Traffic.

Table 26: (Illness) Evaluate MAE of MIA with different pretrained models on multi-variate time series forecasting (MTSF).

Model	Baseline	L_{mask}	$\Delta = 1.0$ 2 %	$\Delta = 1.0$ 5 %	$\Delta = 1.0$ 10 %	$\Delta = 1.2$ 2 %	$\Delta = 1.2$ 5 %	$\Delta = 1.2$ 10 %	$\Delta = 1.5$ 2 %	$\Delta = 1.5$ 5 %	$\Delta = 1.5$ 10 %
MLP-Mixer	0.712	2 %	0.232 **81.3%**			0.251 **86.5%**			0.314 **90.6%**		
		5 %	0.217 77.2%	0.238 76.6%		**0.236** 81.3%	**0.227** 80.7%		**0.309** 88.3%	**0.263** 87.7%	
		10 %	**0.216** 77.2%	**0.220 77.2%**	**0.230 73.1%**	0.254 84.8%	0.252 **84.2%**	**0.247 82.5%**	0.315 88.9%	0.313 **88.9%**	**0.286 88.9%**
MLP	0.930	2 %	0.287 **54.4%**			0.333 **66.1%**			0.394 **82.5%**		
		5 %	**0.258** 51.5%	**0.255 50.9%**		**0.306** 62.6%	**0.301** 61.4%		**0.377** 80.1%	**0.376** 79.5%	
		10 %	0.268 50.9%	0.263 50.3%	**0.256 50.3%**	0.328 65.5%	0.325 **65.5%**	**0.311 63.7%**	0.388 81.9%	0.389 **81.9%**	**0.373 79.5%**
LSTM	1.079	2 %	**0.239 45.6%**			**0.291 59.6%**			0.356 **77.8%**		
		5 %	0.244 **45.6%**	**0.243 45.6%**		0.297 **59.6%**	**0.290 59.6%**		**0.355** 77.2%	**0.348 77.2%**	
		10 %	0.244 **45.6%**	0.243 **45.6%**	**0.239 45.6%**	0.296 **59.6%**	0.296 **59.6%**	**0.292 59.6%**	0.358 77.2%	0.355 76.6%	**0.351 76.6%**
GRU	0.987	2 %	0.300 **54.4%**			0.336 **67.3%**			0.373 **80.1%**		
		5 %	0.296 **54.4%**	0.299 52.0%		0.334 **67.3%**	0.343 66.7%		**0.368** 78.9%	0.373 78.9%	
		10 %	**0.294 54.4%**	**0.294 54.4%**	**0.296 54.4%**	**0.332 67.3%**	**0.331 67.3%**	**0.333 67.3%**	0.374 **80.1%**	**0.373 80.1%**	**0.368 79.5%**
RNN	1.150	2 %	**0.296 38.6%**			0.365 **55.0%**			**0.390 63.7%**		
		5 %	0.300 38.0%	**0.288 38.0%**		0.361 52.6%	**0.353 52.6%**		0.394 63.2%	**0.388 63.2%**	
		10 %	0.297 38.0%	0.297 **38.0%**	**0.293 38.0%**	**0.360** 52.6%	0.357 52.0%	**0.354 52.0%**	0.394 63.2%	0.390 62.6%	**0.387 62.6%**
TransformerNormal	0.877	2 %	0.244 **58.5%**			0.301 **70.2%**			0.376 **82.5%**		
		5 %	0.253 55.0%	0.255 55.0%		0.289 67.8%	0.285 66.7%		0.337 79.5%	**0.327** 78.4%	
		10 %	**0.242** 56.7%	**0.231 55.6%**	**0.232 54.4%**	**0.280** 67.8%	**0.277 67.8%**	**0.272 66.1%**	**0.336** 80.1%	0.330 **79.5%**	**0.326 79.5%**
TransformerPadding	0.945	2 %	**0.290 54.4%**			**0.326 69.0%**			0.362 **84.2%**		
		5 %	0.307 52.6%	0.305 **50.3%**		0.328 66.1%	**0.326** 64.3%		**0.353** 81.3%	**0.358** 81.3%	
		10 %	0.297 50.9%	**0.298** 49.7%	**0.296 48.0%**	0.341 67.3%	0.348 **66.7%**	**0.351 65.5%**	0.372 83.6%	0.374 **82.5%**	**0.381 81.9%**
TransformerConv	0.820	2 %	0.272 **66.1%**			0.316 73.7%			0.395 **80.1%**		
		5 %	0.266 63.2%	0.276 60.8%		0.317 **74.9%**	0.315 **72.5%**		**0.385** 79.5%	**0.372 78.9%**	
		10 %	**0.258** 63.2%	**0.263 61.4%**	**0.263 56.7%**	**0.303** 70.8%	**0.302** 70.2%	**0.309 67.8%**	0.392 78.9%	0.385 **78.9%**	**0.380 77.8%**

Table 27: (Illness) Evaluate MSE of MIA with different pretrained models on multi-variate time series forecasting (MTSF).

Model	Baseline	L_{mask}	$\Delta = 1.0$ 2 %	$\Delta = 1.0$ 5 %	$\Delta = 1.0$ 10 %	$\Delta = 1.2$ 2 %	$\Delta = 1.2$ 5 %	$\Delta = 1.2$ 10 %	$\Delta = 1.5$ 2 %	$\Delta = 1.5$ 5 %	$\Delta = 1.5$ 10 %
MLP-Mixer	0.970	2 %	0.075 **81.3%**			0.095 **86.5%**			0.156 **90.6%**		
		5 %	**0.067** 77.2%	0.076 76.6%		**0.084** 81.3%	**0.078** 80.7%		0.148 88.3%	**0.120** 87.7%	
		10 %	0.069 77.2%	**0.071 77.2%**	**0.075 73.1%**	0.095 84.8%	0.093 **84.2%**	**0.090 82.5%**	**0.148** 88.9%	0.146 **88.9%**	**0.130 88.9%**
MLP	1.265	2 %	0.104 **54.4%**			0.137 **66.1%**			0.203 **82.5%**		
		5 %	**0.085** 51.5%	**0.084 50.9%**		**0.116** 62.6%	**0.112** 61.4%		**0.186** 80.1%	**0.186** 79.5%	
		10 %	0.092 50.9%	0.089 50.3%	**0.086 50.3%**	0.132 65.5%	0.131 **65.5%**	**0.121 63.7%**	0.195 81.9%	0.195 **81.9%**	**0.181 79.5%**
LSTM	1.536	2 %	**0.074 45.6%**			**0.120 59.6%**			0.178 **77.8%**		
		5 %	0.077 **45.6%**	0.076 **45.6%**		0.122 **59.6%**	**0.120 59.6%**		**0.176** 77.2%	**0.172 77.2%**	
		10 %	0.076 **45.6%**	**0.076 45.6%**	**0.074 45.6%**	0.123 **59.6%**	0.123 **59.6%**	**0.121 59.6%**	0.179 77.2%	0.176 76.6%	**0.173 76.6%**
GRU	1.407	2 %	0.114 **54.4%**			0.143 **67.3%**			0.195 **80.1%**		
		5 %	0.110 **54.4%**	0.112 52.0%		0.141 **67.3%**	0.145 66.7%		**0.190** 78.9%	**0.191** 78.9%	
		10 %	**0.109 54.4%**	**0.109 54.4%**	**0.110 54.4%**	**0.140 67.3%**	**0.140 67.3%**	**0.139 67.3%**	0.195 **80.1%**	0.195 **80.1%**	**0.190 79.5%**
RNN	1.727	2 %	**0.111 38.6%**			0.165 **55.0%**			**0.201 63.7%**		
		5 %	0.114 38.0%	**0.106 38.0%**		0.161 52.6%	**0.154 52.6%**		0.203 63.2%	**0.194 63.2%**	
		10 %	0.113 38.0%	0.113 **38.0%**	**0.110 38.0%**	**0.160** 52.6%	0.158 52.0%	**0.155 52.0%**	0.202 63.2%	0.198 62.6%	**0.194 62.6%**
TransformerNormal	1.126	2 %	0.086 **58.5%**			0.126 **70.2%**			0.197 **82.5%**		
		5 %	0.087 55.0%	0.089 55.0%		0.122 67.8%	0.118 66.7%		0.171 79.5%	0.163 78.4%	
		10 %	**0.084** 56.7%	**0.078 55.6%**	**0.078 54.4%**	**0.116** 67.8%	**0.114 67.8%**	**0.110 66.1%**	**0.165** 80.1%	**0.159 79.5%**	**0.157 79.5%**
TransformerPadding	1.236	2 %	**0.115 54.4%**			0.144 **69.0%**			0.187 **84.2%**		
		5 %	0.122 52.6%	0.121 **50.3%**		**0.143** 66.1%	**0.142** 64.3%		**0.183** 81.3%	**0.188** 81.3%	
		10 %	0.119 50.9%	**0.121** 49.7%	**0.120 48.0%**	0.153 67.3%	0.157 **66.7%**	**0.160 65.5%**	0.191 83.6%	0.190 **82.5%**	**0.194 81.9%**
TransformerConv	1.175	2 %	0.105 **66.1%**			0.144 73.7%			0.219 **80.1%**		
		5 %	0.099 63.2%	0.103 60.8%		0.146 **74.9%**	0.143 **72.5%**		**0.210** 79.5%	**0.202 78.9%**	
		10 %	**0.095** 63.2%	**0.097 61.4%**	**0.095 56.7%**	**0.137** 70.8%	**0.137** 70.2%	**0.137 67.8%**	0.215 78.9%	0.210 **78.9%**	**0.206 77.8%**

Table 28: (Weather) Evaluate MAE of MIA with different pretrained models on multi-variate time series forecasting (MTSF).

Model	Baseline	L_{mask}	$\Delta = 1.0$ 2 %	$\Delta = 1.0$ 5 %	$\Delta = 1.0$ 10 %	$\Delta = 1.2$ 2 %	$\Delta = 1.2$ 5 %	$\Delta = 1.2$ 10 %	$\Delta = 1.5$ 2 %	$\Delta = 1.5$ 5 %	$\Delta = 1.5$ 10 %
MLP-Mixer	0.793	2 %	0.362 71.1%			0.440 **78.0%**			0.566 **84.6%**		
		5 %	0.367 **71.5%**	**0.359** 68.7%		0.445 **78.0%**	**0.436** 76.5%		0.571 84.5%	**0.560** 83.3%	
		10 %	**0.362** 70.2%	0.361 **70.0%**	**0.347 66.1%**	**0.439** 77.3%	0.438 **77.3%**	**0.425 74.5%**	**0.563** 84.0%	0.561 **83.9%**	**0.545 82.0%**
MLP	0.831	2 %	**0.405** 70.0%			**0.476** 78.1%			**0.586** 85.9%		
		5 %	0.406 **71.9%**	**0.396** 66.6%		0.478 79.6%	**0.468** 75.1%		0.587 **86.6%**	**0.578** 84.1%	
		10 %	0.405 71.3%	0.402 **70.4%**	**0.389 63.0%**	0.478 **79.8%**	0.475 **79.2%**	**0.461 73.3%**	0.586 86.2%	0.584 **86.2%**	**0.572 84.1%**
LSTM	0.898	2 %	**0.432** 72.3%			**0.516 77.2%**			**0.645 83.6%**		
		5 %	0.432 72.3%	**0.431** 71.8%		0.517 **77.2%**	**0.516** 76.7%		0.646 83.5%	**0.644** 83.0%	
		10 %	0.432 **72.6%**	0.432 **72.3%**	**0.428 71.4%**	0.516 77.0%	0.516 **77.1%**	**0.511 76.5%**	0.646 **83.6%**	0.646 **83.6%**	**0.640 83.2%**
GRU	1.135	2 %	**0.417** 51.7%			**0.514** 63.3%			**0.654** 73.8%		
		5 %	0.419 52.3%	**0.414** 49.8%		0.516 **63.8%**	**0.512** 61.8%		0.655 **74.3%**	**0.652** 72.8%	
		10 %	0.419 **52.4%**	0.417 **52.1%**	**0.410 49.4%**	0.515 63.7%	0.513 **63.3%**	**0.506 59.6%**	0.654 74.1%	0.652 **73.7%**	**0.646 70.9%**
RNN	0.777	2 %	**0.385** 73.1%			**0.465** 77.6%			**0.587** 82.8%		
		5 %	0.388 **74.8%**	**0.367** 71.2%		0.471 79.3%	**0.447** 75.3%		0.593 **83.7%**	**0.568** 79.6%	
		10 %	0.391 74.7%	0.389 **73.6%**	**0.363 65.4%**	0.475 **79.6%**	0.473 **78.7%**	**0.446 72.0%**	0.598 **83.7%**	0.595 **83.1%**	**0.567 77.7%**
TransformerNormal	0.891	2 %	0.412 **68.4%**			0.491 **73.1%**			0.619 **80.0%**		
		5 %	0.412 68.2%	0.409 **66.9%**		0.491 **73.1%**	0.489 **72.6%**		0.616 79.2%	0.614 **78.6%**	
		10 %	**0.406** 66.6%	**0.407** 66.4%	**0.399 65.2%**	**0.485** 72.8%	**0.486** 72.5%	**0.479 71.9%**	**0.609** 78.8%	**0.609** 78.5%	**0.601 77.7%**
TransformerPadding	0.844	2 %	0.392 **70.1%**			0.480 **76.9%**			0.611 **83.5%**		
		5 %	0.392 70.0%	0.387 **69.3%**		0.479 76.5%	0.474 **76.1%**		0.611 83.4%	0.606 **83.2%**	
		10 %	**0.387** 69.5%	**0.385** 69.0%	**0.382 68.2%**	**0.474** 76.3%	**0.473** 76.0%	**0.469 75.5%**	**0.604** 82.8%	**0.603** 82.7%	**0.600 82.6%**
TransformerConv	0.886	2 %	0.394 **66.9%**			0.475 **74.5%**			0.598 **82.3%**		
		5 %	0.393 66.6%	0.391 **66.1%**		0.475 74.3%	0.472 **73.7%**		0.598 82.2%	0.596 **81.6%**	
		10 %	**0.389** 65.6%	**0.388** 65.5%	**0.384 63.9%**	**0.468** 72.4%	**0.466** 72.0%	**0.459 70.5%**	**0.592** 81.4%	**0.592** 81.1%	**0.582 79.9%**

Table 29: (Weather) Evaluate MSE of MIA with different pretrained models on multi-variate time series forecasting (MTSF).

Model	Baseline	L_{mask}	$\Delta = 1.0$ 2 %	$\Delta = 1.0$ 5 %	$\Delta = 1.0$ 10 %	$\Delta = 1.2$ 2 %	$\Delta = 1.2$ 5 %	$\Delta = 1.2$ 10 %	$\Delta = 1.5$ 2 %	$\Delta = 1.5$ 5 %	$\Delta = 1.5$ 10 %
MLP-Mixer	1.227	2 %	0.159 71.1%			0.235 **78.0%**			0.378 **84.6%**		
		5 %	0.162 **71.5%**	**0.157** 68.7%		0.238 **78.0%**	**0.232** 76.5%		0.383 84.5%	**0.373** 83.3%	
		10 %	**0.159** 70.2%	0.158 **70.0%**	**0.149** **66.1%**	**0.234** 77.3%	0.233 **77.3%**	**0.222** **74.5%**	**0.376** 84.0%	0.375 **83.9%**	**0.359** **82.0%**
MLP	1.485	2 %	**0.187** 70.0%			**0.262** 78.1%			**0.403** 85.9%		
		5 %	0.187 **71.9%**	**0.180** 66.6%		0.263 79.6%	**0.255** 75.1%		0.405 **86.6%**	**0.395** 84.1%	
		10 %	0.187 71.3%	0.184 **70.4%**	**0.176** **63.0%**	0.263 **79.8%**	0.261 **79.2%**	**0.250** **73.3%**	0.404 86.2%	0.402 **86.2%**	**0.390** **84.1%**
LSTM	1.900	2 %	**0.204** 72.3%			**0.293** **77.2%**			**0.455** **83.6%**		
		5 %	0.204 72.3%	**0.204** 71.8%		0.293 **77.2%**	**0.292** 76.7%		0.456 83.5%	**0.455** 83.0%	
		10 %	0.205 **72.6%**	0.204 **72.3%**	**0.202** **71.4%**	0.293 77.0%	0.293 **77.1%**	**0.289** **76.5%**	0.456 **83.6%**	0.456 **83.6%**	**0.451** **83.2%**
GRU	2.167	2 %	**0.194** 51.7%			**0.290** 63.3%			**0.465** 73.8%		
		5 %	0.195 52.3%	**0.192** 49.8%		0.292 **63.8%**	**0.289** 61.8%		0.467 **74.3%**	0.464 72.8%	
		10 %	0.195 **52.4%**	0.194 **52.1%**	**0.189** **49.4%**	0.291 63.7%	0.290 **63.3%**	**0.283** **59.6%**	0.466 74.1%	**0.464** **73.7%**	**0.457** **70.9%**
RNN	1.591	2 %	**0.171** 73.1%			**0.249** 77.6%			**0.392** 82.8%		
		5 %	0.173 **74.8%**	**0.160** 71.2%		0.252 79.3%	**0.234** 75.3%		0.397 **83.7%**	**0.371** 79.6%	
		10 %	0.176 74.7%	0.174 **73.6%**	**0.158** **65.4%**	0.256 **79.6%**	0.253 **78.7%**	**0.234** **72.0%**	0.402 **83.7%**	0.399 **83.1%**	**0.371** **77.7%**
TransformerNormal	1.457	2 %	0.190 **68.4%**			0.272 **73.1%**			0.432 **80.0%**		
		5 %	0.190 68.2%	0.189 **66.9%**		0.272 **73.1%**	0.271 **72.6%**		0.430 79.2%	0.427 **78.6%**	
		10 %	**0.187** 66.6%	**0.187** 66.4%	**0.182** **65.2%**	**0.268** 72.8%	**0.268** 72.5%	**0.262** **71.9%**	**0.423** 78.8%	**0.422** 78.5%	**0.414** **77.7%**
TransformerPadding	1.502	2 %	0.178 **70.1%**			0.263 **76.9%**			0.418 **83.5%**		
		5 %	0.178 70.0%	0.175 **69.3%**		0.262 76.5%	0.258 **76.1%**		0.418 83.4%	0.413 **83.2%**	
		10 %	**0.175** 69.5%	**0.174** 69.0%	**0.171** **68.2%**	**0.258** 76.3%	**0.257** 76.0%	**0.255** **75.5%**	**0.411** 82.8%	**0.410** 82.7%	**0.407** **82.6%**
TransformerConv	1.599	2 %	0.179 **66.9%**			0.261 **74.5%**			0.410 **82.3%**		
		5 %	0.179 66.6%	0.178 **66.1%**		0.261 74.3%	0.259 **73.7%**		0.410 82.2%	0.407 **81.6%**	
		10 %	**0.176** 65.6%	**0.175** 65.5%	**0.171** **63.9%**	**0.256** 72.4%	**0.254** 72.0%	**0.248** **70.5%**	**0.405** 81.4%	**0.404** 81.1%	**0.395** **79.9%**

Table 30: Compare ℓ_0-norm localized perturbation to ℓ_2-norm perturbation (computed by the algorithm [2]) on the MSE between the original forecast and the perturbed forecast. The table reports the relative improvement of the ℓ_0-norm perturbation over the ℓ_2-norm perturbation (averaging among 128 randomly selected samples). The positive value indicates that our ℓ_0-norm perturbation outperforms ℓ_0-norm perturbation. For fairness, the ℓ_0 or ℓ_2 norm of the perturbation is restricted to be no larger than $\boldsymbol{\beta}\times$ the average value among the ℓ_0 or ℓ_2 norm of all the testing samples. Values in tables are calculated as $(\text{MSE}_{\ell_0} - \text{MSE}_{\ell_2})/\text{MSE}_{\ell_2}$.

Model	Attack Rate (β) 10 %	20 %	30 %	40 %	50 %
MLP-Mixer	+769.9 %	+89.5 %	+73.3 %	+12.3 %	+53.1 %
GRU	+2.5 %	-1.6 %	-8.3 %	-3.3 %	-6.5 %
LSTM	+23.1 %	+15.1 %	-33.5 %	-14.8 %	+2.0 %
MLP	+265.0 %	+376.3 %	+211.6 %	+114.1 %	+58.3 %

Table 31: (Exchange) Time series attack. Difference of MSE between ℓ_0 and ℓ_2 attack.

Model	Attack Rate (β) 10 %	20 %	30 %	40 %	50 %
MLP-Mixer	+1000.1 %	+332.2 %	+114.7 %	+131.7 %	+84.6 %
GRU	-48.6 %	-45.1 %	-39.7 %	-31.7 %	-20.9 %
LSTM	-8.8 %	-28.3 %	-24.9 %	-16.2 %	-6.6 %
MLP	+528.9 %	+101.8 %	+36.9 %	+8.8 %	+6.2 %

Table 32: (Traffic) Time series attack. Difference of MSE between ℓ_0 and ℓ_2 attack.

Model	Attack Rate (β) 10 %	20 %	30 %	40 %	50 %
MLP-Mixer	+3310.1 %	+841.8 %	+328.5 %	+317.7 %	+205.5 %
GRU	+147.0 %	+28.2 %	+7.3 %	-4.7 %	+21.6 %
LSTM	+239.0 %	+66.8 %	+14.9 %	+2.5 %	-2.8 %
MLP	+1760.4 %	+145.7 %	+38.4 %	+7.5 %	-7.6 %

Table 33: (DistalPhalanxTW $L_{mask} = 15\%$) $\sigma = 0.01$

Model	Metric, $\sigma = 0.010$	L_{mask}	DistalPhalanxTW			MiddlePhalanxTW			ProximalPhalanxTW		
			5 %	10 %	15 %	5 %	10 %	15 %	5 %	10 %	15 %
FCN	ACC	5 %	1.0 %			-3.0 %			0.0 %		
		10 %	-1.0 %	0.0 %		0.0 %	-1.0 %		-1.0 %	-3.0 %	
		15 %	1.0 %	3.0 %	0.0 %	-4.0 %	-3.0 %	-4.0 %	-1.0 %	1.0 %	3.0 %
MLP-Mixer	ACC	5 %	0.0 %			0.0 %			1.0 %		
		10 %	-2.0 %	-2.0 %		0.0 %	-1.0 %		-1.0 %	-1.0 %	
		15 %	-2.0 %	0.0 %	-2.0 %	-1.0 %	1.0 %	-2.0 %	1.0 %	0.0 %	2.0 %
MLP	ACC	5 %	-1.0 %			2.0 %			0.0 %		
		10 %	-1.0 %	-1.0 %		-1.0 %	0.0 %		0.0 %	0.0 %	
		15 %	1.0 %	1.0 %	3.0 %	2.0 %	4.0 %	2.0 %	1.0 %	0.0 %	0.0 %
ResNet-18	ACC	5 %	-2.0 %			-1.0 %			0.0 %		
		10 %	3.0 %	0.0 %		0.0 %	0.0 %		0.0 %	1.0 %	
		15 %	-1.0 %	-3.0 %	-1.0 %	0.0 %	1.0 %	1.0 %	-1.0 %	-2.0 %	-1.0 %

Table 34: (DistalPhalanxTW $L_{mask} = 15\%$) $\sigma = 0.02$

Model	Metric, $\sigma = 0.020$	L_{mask}	DistalPhalanxTW			MiddlePhalanxTW			ProximalPhalanxTW		
			5 %	10 %	15 %	5 %	10 %	15 %	5 %	10 %	15 %
FCN	ACC	5 %	-1.0 %			0.0 %			0.0 %		
		10 %	0.0 %	1.0 %		0.0 %	0.0 %		0.0 %	0.0 %	
		15 %	5.0 %	6.9 %	3.0 %	0.0 %	-1.0 %	-2.0 %	0.0 %	1.0 %	2.0 %
MLP-Mixer	ACC	5 %	0.0 %			1.0 %			1.0 %		
		10 %	1.0 %	0.0 %		0.0 %	2.0 %		1.0 %	-1.0 %	
		15 %	-1.0 %	3.0 %	5.0 %	2.0 %	0.0 %	0.0 %	0.0 %	0.0 %	0.0 %
MLP	ACC	5 %	0.0 %			2.0 %			0.0 %		
		10 %	3.0 %	0.0 %		1.0 %	2.0 %		0.0 %	1.0 %	
		15 %	0.0 %	2.0 %	3.0 %	2.0 %	3.0 %	3.0 %	0.0 %	0.0 %	0.0 %
ResNet-18	ACC	5 %	-3.0 %			0.0 %			0.0 %		
		10 %	5.0 %	1.0 %		-1.0 %	1.0 %		0.0 %	0.0 %	
		15 %	0.0 %	1.0 %	1.0 %	1.0 %	2.0 %	2.0 %	0.0 %	-1.0 %	-1.0 %

Table 35: (DistalPhalanxTW $L_{mask} = 15\%$) $\sigma = 0.03$

Model	Metric, $\sigma = 0.030$	L_{mask}	DistalPhalanxTW			MiddlePhalanxTW			ProximalPhalanxTW		
			5 %	10 %	15 %	5 %	10 %	15 %	5 %	10 %	15 %
FCN	ACC	5 %	-2.0 %			0.0 %			1.0 %		
		10 %	-2.0 %	0.0 %		-1.0 %	-3.0 %		-3.0 %	-2.0 %	
		15 %	2.0 %	3.0 %	2.0 %	-2.0 %	-3.0 %	-2.0 %	-1.0 %	2.0 %	2.0 %
MLP-Mixer	ACC	5 %	0.0 %			1.0 %			2.0 %		
		10 %	0.0 %	1.0 %		-1.0 %	1.0 %		1.0 %	0.0 %	
		15 %	-1.0 %	3.0 %	3.0 %	1.0 %	0.0 %	0.0 %	1.0 %	1.0 %	0.0 %
MLP	ACC	5 %	0.0 %			2.0 %			0.0 %		
		10 %	1.0 %	1.0 %		0.0 %	1.0 %		0.0 %	1.0 %	
		15 %	1.0 %	3.0 %	4.0 %	0.0 %	1.0 %	1.0 %	-1.0 %	0.0 %	-1.0 %
ResNet-18	ACC	5 %	-4.0 %			2.0 %			0.0 %		
		10 %	0.0 %	-1.0 %		0.0 %	1.0 %		0.0 %	1.0 %	
		15 %	-1.0 %	-1.0 %	0.0 %	0.0 %	1.0 %	1.0 %	0.0 %	0.0 %	0.0 %

Table 36: (DistalPhalanxTW $L_{mask} = 15\%$) $\sigma = 0.04$

Model	Metric, $\sigma = 0.040$	L_{mask}	DistalPhalanxTW			MiddlePhalanxTW			ProximalPhalanxTW		
			5 %	10 %	15 %	5 %	10 %	15 %	5 %	10 %	15 %
FCN	ACC	5 %	2.0 %			-1.0 %			0.0 %		
		10 %	2.0 %	3.0 %		-2.0 %	-2.0 %		-2.0 %	-2.0 %	
		15 %	2.0 %	1.0 %	0.0 %	-1.0 %	-2.0 %	-2.0 %	-3.0 %	1.0 %	1.0 %
MLP-Mixer	ACC	5 %	-1.0 %			1.0 %			0.0 %		
		10 %	0.0 %	1.0 %		0.0 %	-1.0 %		0.0 %	0.0 %	
		15 %	0.0 %	2.0 %	0.0 %	0.0 %	1.0 %	-2.0 %	-1.0 %	2.0 %	0.0 %
MLP	ACC	5 %	1.0 %			1.0 %			1.0 %		
		10 %	1.0 %	0.0 %		0.0 %	1.0 %		1.0 %	1.0 %	
		15 %	1.0 %	3.0 %	4.0 %	1.0 %	3.0 %	3.0 %	-1.0 %	0.0 %	0.0 %
ResNet-18	ACC	5 %	-1.0 %			1.0 %			-1.0 %		
		10 %	0.0 %	0.0 %		0.0 %	1.0 %		1.0 %	1.0 %	
		15 %	2.0 %	2.0 %	0.0 %	1.0 %	1.0 %	2.0 %	0.0 %	0.0 %	-1.0 %

Table 37: (DistalPhalanxTW $L_{mask} = 15\%$) $\sigma = 0.05$

Model	Metric, $\sigma = 0.050$	L_{mask}	DistalPhalanxTW			MiddlePhalanxTW			ProximalPhalanxTW		
			5 %	10 %	15 %	5 %	10 %	15 %	5 %	10 %	15 %
FCN	ACC	5 %	1.0 %			0.0 %			1.0 %		
		10 %	0.0 %	1.0 %		-1.0 %	-4.0 %		-1.0 %	0.0 %	
		15 %	5.0 %	4.0 %	2.0 %	0.0 %	-1.0 %	-2.0 %	0.0 %	2.0 %	1.0 %
MLP-Mixer	ACC	5 %	-1.0 %			-2.0 %			1.0 %		
		10 %	1.0 %	1.0 %		-2.0 %	-1.0 %		-1.0 %	-2.0 %	
		15 %	2.0 %	5.0 %	0.0 %	3.0 %	1.0 %	0.0 %	0.0 %	-1.0 %	2.0 %
MLP	ACC	5 %	1.0 %			2.0 %			0.0 %		
		10 %	4.0 %	1.0 %		-1.0 %	1.0 %		0.0 %	0.0 %	
		15 %	2.0 %	3.0 %	3.0 %	2.0 %	4.0 %	1.0 %	-1.0 %	0.0 %	0.0 %
ResNet-18	ACC	5 %	-2.0 %			0.0 %			-1.0 %		
		10 %	3.0 %	-1.0 %		-1.0 %	-1.0 %		0.0 %	-1.0 %	
		15 %	1.0 %	1.0 %	0.0 %	1.0 %	1.0 %	1.0 %	-1.0 %	0.0 %	-1.0 %

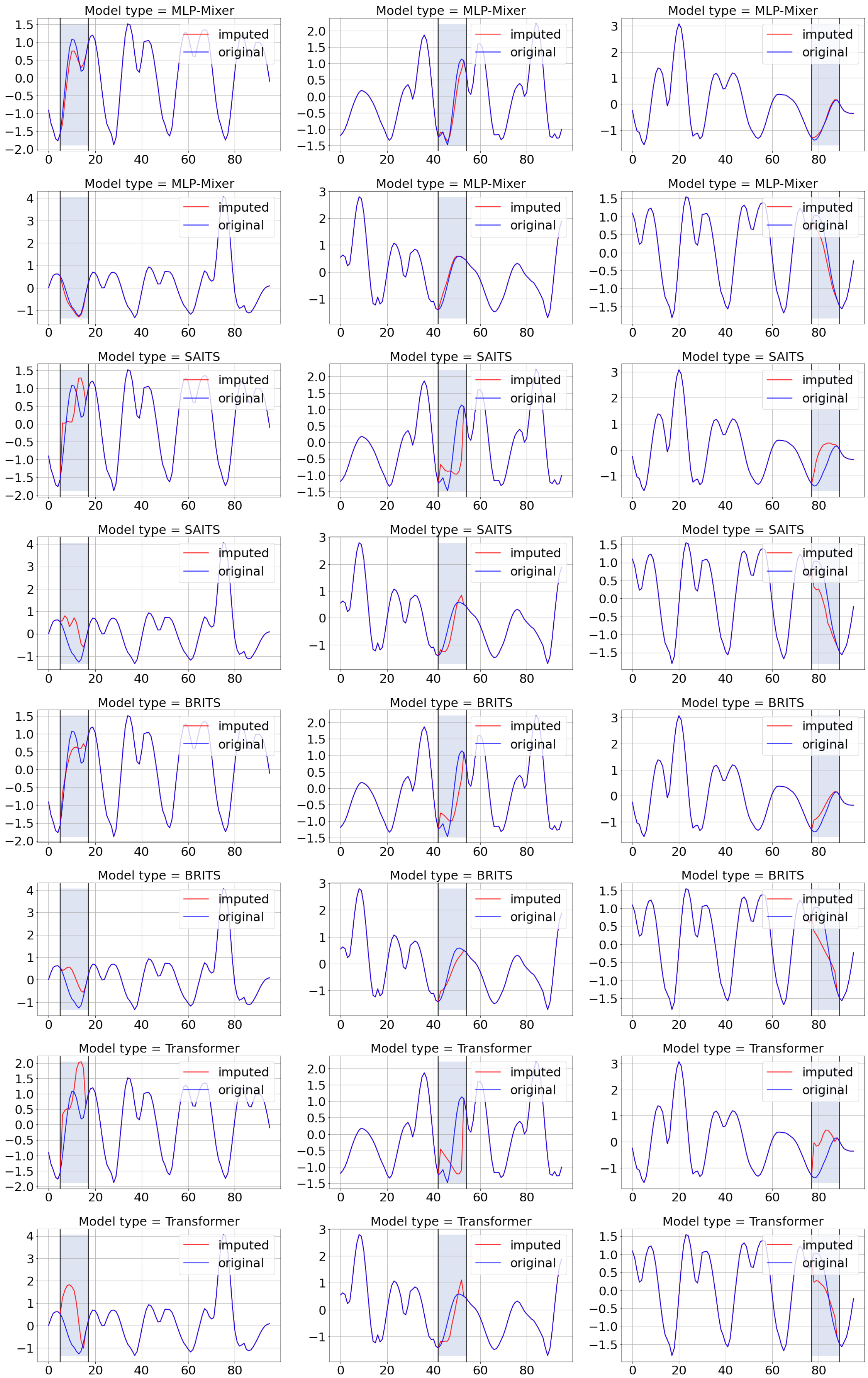

Figure 4: (Traffic) Imputation quality with different imputation models. We set $L_{\text{mask}} = 10\%$. Original and imputed refer to the original time series and the imputed time series respectively.